People's Democratic Republic of Algeria
Ministry of Higher Education and Scientific Research

University M'Hamed BOUGARA – Boumerdes

Institute of Electrical and Electronic Engineering
Department of Power and Control

Final Year Project Report Presented in Partial Fulfilment of the Requirements for the Degree of

MASTER

In **Control**

Option: **Control**

Title:

Design and Implementation of Speed and Torque controller for DC motor

Presented by:

- **BELHOUT Saber**
- **ROUARI Baha Eddine**

Supervisor:

Pr. BENTARZI Hamid

Registration Number:……/2018

Abstract

Electric drives have many applications in different areas such as industry, transport, agriculture and domestic. The operation of electric drives are selectively regulated and made partly or fully automatic to increase the productivity and efficiency of the industry. The dc drives still play a significant role in modern industrial drives due to its higher performance, reliability, adjustable speed control etc. This project aim is to design and implement a speed and current controller for PMDC motor with a high performance. Using the chopper as a converter, the speed of DC motor may be controllable. The chopper firing circuit may get signal from controller in order to supply variable voltage to the armature of the DC motor at the desired speed. The controller consists of two different control loops, current control and speed control. The used controller is Proportional-Integral type due to its fastness. The current and speed controller is designed by taking into consideration the high stability even at high speed control of DC motor. The simulation of model is investigated and analyzed using LABVIEW and Simulink/MATLAB under different speed and torque conditions.

DEDICATION

I would like to dedicate this work:

To My beloved Mother and Father, my sister & my brothers especially the little one Yakoub

To All dear friends , whoever helped to achieve this work , To Cylia.

Baha Eddine

I would like to dedicate this work:

To My beloved Mother,

To All dear friends,

students and whoever helped to achieve this work

Saber

ACKNOWLEDGEMENTS

We would like to start by thanking ALLAH, without his graciousness the completion of this work would not have been possible. We would like to thank our supervisor, ***Pr. BENTARZI HAMID*** *as well for his continuous encouragement, invaluable supervision, timely suggestions and inspired guidance throughout the completion of this thesis. Special thanks to our friends surrounding us especially our beloved classmates.*

Finally, we extend our gratitude to one and all who are directly or indirectly involved in the successful completion of this thesis.

TABLE OF CONTENTS

LIST OF TABLES

LIST OF FIGURES

CHAPTER 1: MODELING OF DC MACHINES

CHAPTER 2: DC CHOPPER

CHAPTER 3: OPEN LOOP AND CLOSED LOOP CONTROLLER

CHAPTER 4: SYSTEM PARAMETERS IDENTIFICATION

CHAPTER 5: IMPLEMENTATION OF LABVIEW BASED CONTROLLER

LIST OF ABBREVIATIONS AND ACRONYMS

AC	Alternative Current
DC	Direct Current
EMF	Electromotive force
PMDC	permanent magnet direct current
SCR	silicon-controlled rectifier
FD	Freewheeling diode
BJT	Bipolar Junction Transistor
MOSFET	Metal-Oxide-Semiconductor-Field-Effect-Transistor
PWM	Pulse Width Modulation
DCS	Discrete Control System
PI	proportional-integral controller
PID	proportional-integral-derivative controller
SP	set-point
PV	process variable
CT	Continuous Time
SMPS	Switch Mode Power Supply
V_a	voltage across the coil of the armature
L_a	The inductance of the armature winding E_c
R_a	The resistance of the armature winding E_c
K_v	Motor voltage constant
w_m	The rotational velocity of the armature
I_a	The current flowing in the armature circuit
T_e	The electromagnetic torque
$T_{\omega'}$	The torque due to rotational acceleration of the rotor
T_ω	The torque produced from the velocity of the rotor
T_l	The torque of the mechanical load
K_t	The torque constant
J	The inertia of the rotor
B	The damping coefficient

V_s	Supply Voltage
V_o	Output Voltage
T	switching period
α	Duty cycle
T_{ON}	Time when switch is open
T_{OFF}	Time when switch is closed
fs	Switching Frequency
i_L	The current through the inductor
V_c	The voltage across the capacitor
t_d	Delay time
t_r	Rise time
t_p	Peak time
M_p	Maximum (percent) overshoot
t_s	Settling time
p_{out}	Proportional output
I_o	the current through the load
V	Voltage
d/dt	first derivative with respect to time
Δ/Δt	rate of change
V_T	The voltage applied across the motor terminals
E_c	The total voltage induced in the armature
E(s)	The error
u(t)	The controller output
e(t)	the error
K_p	Proportional gain
K_i	Integral gain
K_d	Derivative gain

Introduction

In a modern industrial situation, DC motor is widely used due to the low initial cost, excellent drive performance, low maintenance and the noise limit. As the electronic technology develops rapidly, it provides a wide range of applications of high performance DC motor drives in areas such as rolling mills, electric vehicle tractions, electric trains, electric bicycles, guided vehicles, robotic manipulators, and home electrical appliances.

DC motors have some control capabilities, which means that speed, torque and even direction of rotation can be changed at any time to meet new condition. DC motors also can provide a high starting torque at low speed and it is possible to obtain speed control over a wide range. So, the study of DC motor controller is more practical significant.

Control theory is an interdisciplinary area of engineering and mathematics that deals with the dynamical behavior of systems. For controlling a motor in any system, a controller is needed which is to give input to gate driver. For motor actuation, the microcontroller does not directly actuate the DC motor but it will actuate it through the use of a device known as gate driver. In this system, PWM amplifier may be used to provide variable output voltage for controlling the speed of the motor as well as its direction by applying positive or negative voltage.

I. Modeling of DC machines

1.1 Introduction

A DC motor is a machine that converts electrical energy into mechanical energy. The operation is based on simple electromagnetism, i.e. "when a current carrying conductor is placed in an external magnetic field it experiences a force which is proportional to the current and the external magnetic field". A torque is developed by the magnetic reaction and the armature revolves and this induces a voltage in the armature windings which is opposite in direction to the outside voltage applied to the armature, when current is passed through the armature of the DC motor, and hence is called back voltage or counter EMF. The back voltage rises till it becomes equal to the applied voltage as the motor rotates faster. [12]

1.2 Physical Construction Description

A very basic permanent magnet PMDC motor is constructed of two main components: the armature (rotor) including armature winding and the stator made from permanent magnet. The armature rotates within the framework of the stationary part called stator. A simple illustration of a dc motor is given in Figure 1. 1.

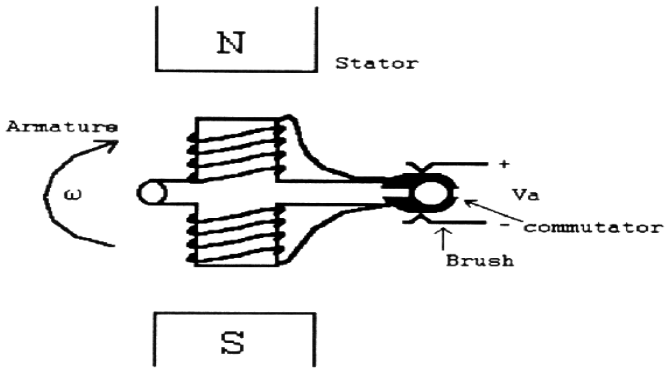

Figure 1. 1: Basic dc motor configuration.

The stator creates a magnetic field. However, the armature winding creates an electromagnetic field. The rotor (armature) rotates due to the phenomenon of attracting and opposing forces of the two magnetic fields. A magnetic field is generated by the armature by sending an electrical current through the coil and the polarity is constantly changed by alternating the current through the coil (also known as commutation) causing the armature to rotate. The commutator is made up of two semicircular copper segments mounted on the

shaft at the end of the rotor. Each terminal of the rotor coil is connected to a copper segment. Stationary brushes ride on the copper segments whereby the rotor coil is connected to a stationary dc voltage supply by a near frictionless contact. [13]

1.3 Mathematical Model

The goal in the development of the mathematical model is to relate the voltage applied to the armature to the velocity of the motor. Two balance equations can be developed by considering the electrical and mechanical characteristics of the system. [14]

1.3.1 Characteristics

Electrical Characteristics

The electrical equivalent circuit of a dc motor is illustrated in Fig. 1.2. It can be represented by a voltage source (V_a) across the coil of the armature. The electrical equivalent of the armature coil can be described by an inductance (L_a) in series with a resistance (R_a) in series with an induced voltage (E_c) which opposes the applied voltage. The induced voltage is generated by the rotation of the electrical coil through the fixed flux lines of the permanent magnets. This voltage is often referred to as the back-EMF (electromotive force). [14]

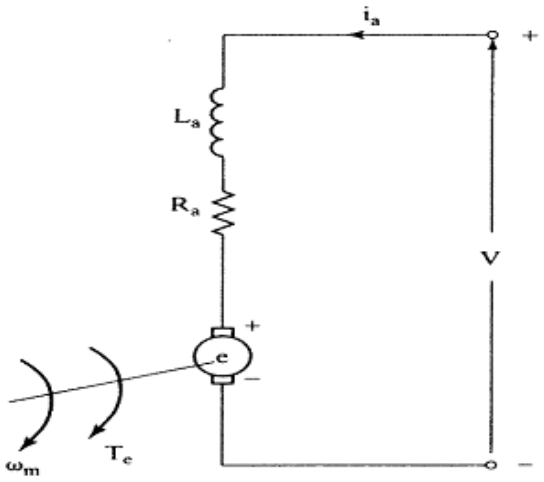

Figure 1.2: Equivalent circuit of PMDC motor.

A differential equation for the equivalent circuit can be derived by using Kirchhoff's voltage law around the electrical loop, or

$$V_a = R_a i_a + L_a \frac{di_a}{dt} + E_C \tag{1.1}$$

Where the motor back EMF, is expressed as follows:

$$E_C = K_v \omega_m \tag{1.2}$$

Where:

i_a: The armature current.

ω_m: The rotational velocity of the armature, [rad/sec].

K_v : Motor voltage constant [v/amp-rad/sec].determined by the flux density of the permanent magnets, the reluctance of the iron core of the armature, and the number of turns of the armature winding. [14]

Mechanical Characteristics

Performing an energy balance on the system, the sum of the torques of the motor must equal zero. Therefore,

$$T_e - T_{\omega'} - T_\omega - T_l = 0 \tag{1.3}$$

Where T_e is the electromagnetic torque, $T_{\omega'}$ is the torque due to rotational acceleration of the rotor, T_ω is the torque produced from the velocity of the rotor, and T_l is the torque of the mechanical load. The electromagnetic torque is proportional to the current through the armature winding and can be written as:

$$T_e = K_t i_a \tag{1.4}$$

Where K_t is the torque constant and like the voltage constant is dependent on the flux density of the fixed magnets, the reluctance of the iron core, and the number of turns in the armature winding. $T_{\omega'}$ can be written as

$$T_{\omega'} = J \frac{d\omega_m}{dt} \tag{1.5}$$

Where J is the inertia of the rotor and the equivalent mechanical load. The torque associated with the velocity is written as

$$T_{\omega} = B\omega_m \tag{1.6}$$

Where B is the damping coefficient associated with the mechanical rotational system of the machine. [14]

Substituting eqns. (1.4), (1.5), and (1.6) into eqn. (1.3) then the torque developed by the motor is:

$$T_e = K_t i_a = J\frac{d\omega_m}{dt} + B\omega_m + T_l \tag{1.7}$$

1.3.2 State Space Representation

The differential equations for the armature current and the angular velocity can be obtained from rearrangement of Eqns. (1.1) and (1.7):

$$\frac{d\omega_m}{dt} = \frac{K_t}{J} i_a - \frac{B}{J}\omega_m - \frac{T_l}{J} \tag{1.8}$$

$$\frac{di_a}{dt} = -\frac{R_a}{L_a} i_a - \frac{K_v}{L_a}\omega_m + \frac{V_a}{L_a} \tag{1.9}$$

Which describe the dc motor system. Converting the differential equations (1.8) and (1.9) to state space form gives:

$$\begin{pmatrix} \frac{di_a}{dt} \\ \frac{d\omega_m}{dt} \end{pmatrix} = \begin{pmatrix} -\frac{R_a}{L_a} & -\frac{K_v}{L_a} \\ \frac{K_t}{J} & -\frac{B}{J} \end{pmatrix} \begin{pmatrix} i_a \\ \omega_m \end{pmatrix} + \begin{pmatrix} \frac{1}{L_a} & 0 \\ 0 & -\frac{1}{J} \end{pmatrix} \begin{pmatrix} V_a \\ T_l \end{pmatrix} \tag{1.10}$$

Equation (1.10) is expressed compactly in the form:

$$\dot{X} = AX + BU \tag{1.11}$$

Where:

$$X = \begin{pmatrix} i_a \\ \omega_m \end{pmatrix}; \dot{X} = \begin{pmatrix} \frac{di_a}{dt} \\ \frac{d\omega_m}{dt} \end{pmatrix}; A = \begin{pmatrix} -\frac{R_a}{L_a} & -\frac{K_v}{L_a} \\ \frac{K_t}{J} & -\frac{B}{J} \end{pmatrix}; B = \begin{pmatrix} \frac{1}{L_a} & 0 \\ 0 & -\frac{1}{J} \end{pmatrix}; U = \begin{pmatrix} V_a \\ T_l \end{pmatrix}$$

1.3.3 Block diagrams and transfer functions

The block diagram of Permanent magnet DC motor is shown in Fig.1.3.

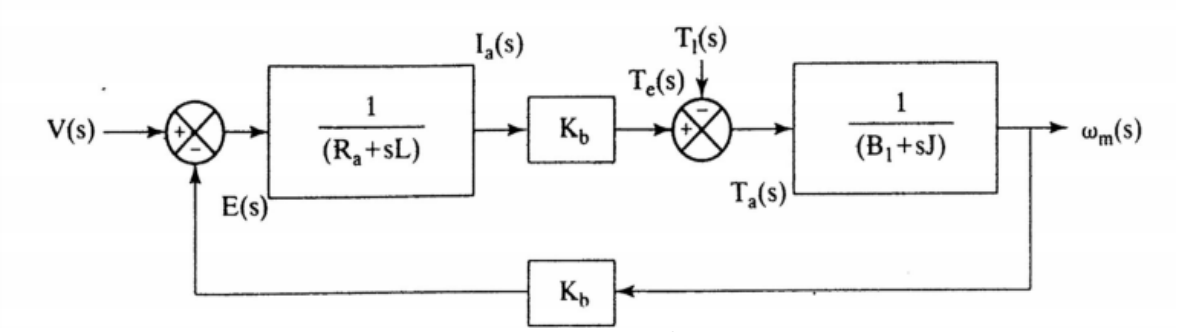

Figure 1.3: Block diagram of PMDC motor.

Taking Laplace transform of equations (1.8) and (1.9) and making initial conditions equal to zero, we get:

$$i_a(s) = \frac{V_a(s) - K_v\omega_m(s)}{R_a + sL_a} \tag{1.12}$$

$$\omega_m(s) = \frac{-K_t i_a(s) - T_l(s)}{B + sJ} \tag{1.13}$$

In block diagram form, the relationships are represented in figure (1.3) .Then, the transfer functions are derived from the block diagram as

$$G(s) = \frac{\omega_m(s)}{V_a(s)} = \frac{K_t}{s^2(JL_a) + s(BL_a + JR_a) + (BR_a + K_tK_v)} \tag{1.14}$$

$$H(s) = \frac{\omega_m(s)}{T_l(s)} = \frac{-(sL_a + R_a)}{s^2(JL_a) + s(BL_a + JR_a) + (BR_a + K_tK_v)} \tag{1.15}$$

The PMDC motor is a linear system, and hence the speed response $\omega_m(s)$ due to the simultaneous voltage input and load torque disturbance can be written as a sum of their individual responses:

$$\omega_m(s) = H(s)T_l(s) + G(s)V_a(s) \tag{1.16}$$

Laplace inverse of equation (1.16) gives the time response of the speed for a simultaneous change in the input voltage and load torque. [14]

1.4 Approach for characterizing a dc motor

The conventional way of characterizing a dc motor is to perform a separate test for each parameter, but this is not only time consuming, but can yield misleading results if the parameters are measured under static or no load conditions. So, other methods have been developed get accurate parameters need for good controlling. There are various

methods such as Pasek's frequency response, pseudo inverse and nonlinear least square method. [15]

Pasek's method is one of the earliest techniques used in parameters identification of dc motors. It determines a high-performance dc motor's mode model type and all the model parameters based only on the current response of the machine to a step input of armature voltage along with the steady state speed. But this method can introduce some instrumentation problems. The technique requires an accurate reading of two points of transient waveform, which can be difficult to do in presence of noise. Also this method measures a few points on the current time response curve making it is very sensitive to current commutation noise, which renders the method in accurate for low cost dc motors widely used in our industry. [15]

An alternative method to Pasek's method is the frequency response method for determining the parameters of high performance dc motors. This method has the following features:

1. All significant motor parameters are determined at once in a dynamic and loaded condition.
2. No nonelectrical measurements are required (such as speed in Pasek's method).
3. Results are averaged out to minimize errors caused by noise.
4. Sophisticated instrumentation is not necessary.
5. The approach is readily adaptable to automatic testing.

Frequency response method determines the parameters of high performance dc motors by treating a second order motor model as an electrical impedance (RLC circuit), and by tuning the values of RLC circuit elements to match the response of dc motor and by some relations the parameters of dc motor are calculated. [15]

This method uses an AC signal with specific frequency about 1kHz. Unfortunately, this method is not suitable to the power drivers used in our experimental platform; sensitivity to noise is another reason that discouraged us to utilize this method. [15]

The pseudo inverse technique is a method capable of identifying an equivalent discrete transfer function of simple systems like motor, thermal system, mass damper systems etc. with no zeros(only poles). This method assumes a single input single output system and unable to find the dc motor parameters and doesn't fit our objective. [10]

Nonlinear least square method is a general approach in identification seeks to define an objective function that would reach its minimum. The physical system to be investigated is described in terms of parameters, and then, the objective function is minimized with respect to the parameters by an iterative procedure. At the minimum of the objective function, the values of the parameters describe the real structure of the physical system. [11]

Pattern search algorithm is another method used in this thesis and applied practically on our experimental system. Pattern search is an attractive alternative to the genetic algorithm, as it is often computationally less expensive and can minimize the same types of functions. Finally, this method can be used to find the motor parameters with less error and compare it with previous methods. [11]

1.5 Applications of DC motors

Permanent magnet dc motors are extensively used where smaller power ratings are required, e.g. in toys, small robots, computer disc drives etc. [16]

1.6 Advantages and Disadvantages

1.6.1 Advantages

The D.C motors have the following main advantages [16]:

1. For smaller ratings, use of permanent magnets reduces manufacturing cost.

2. No need of field excitation winding, hence construction is simpler.

3. No need of electrical supply for field excitation, hence PMDC motor is relatively more efficient.

4. Relatively smaller in size.

5. Cheap in cost.

1.6.2 Disadvantages

The main disadvantages of D.C motors are [16]:

1. Since the stator in PMDC motor consists of permanent magnets, it is not possible to add extra ampere-turns to reduce armature reaction. Thus armature reaction is more in PMDC motors.

2. Stator side field control, for controlling speed of the motor, is not possible in permanent magnet dc motors.

II. DC chopper

1. Introduction
2. Chopper-definitions
3. Principle of operation
4. Classification of choppers
5. Class E chopper operation
6. Applications of choppers

2.1 Introduction

The Choppers or DC–DC converters can be operated in either a continuous or discontinuous current conduction mode, they can be built with and without electrical isolation. [17]

2.2 Chopper – Definition

A chopper is a static device that converts fixed dc input voltage to a variable dc output voltage directly. [17]

- A chopper is considered as DC equivalent of an AC transformer since it behaves in an identical manner.
- The choppers are more efficient as they involve in one stage conversion.
- The choppers are used in trolley cars, marine hoists, forklift trucks and mine hauler.
- The future electric automobiles are likely to use choppers for their speed control and braking.
- The chopper systems offer smooth control, high-efficiency, fast response and regeneration.
- The chopper is the dc equivalent to an AC transformer having continuously variable turn's ratio. Like a transformer, a chopper can be used to step down or step up the fixed dc input voltage.

2.3 Principle of operation

A chopper is a high speed ON/OFF semiconductor switch. Figure 2.1 shows a chopper schematic diagram. It connects source to load and disconnects the load from source at high speed. A chopped load voltage is obtained from a constant DC supply of magnitude V_s. [18]

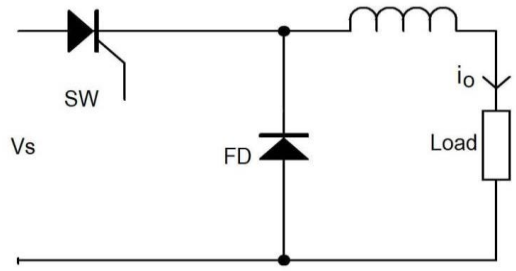

Figure 2.1: A chopper schematic diagram.

The principle of chopper operation can be explained in figures 2.2 and 2.3.

Here the SCR (silicon-controlled rectifier) is used as a switch. The SCR can be turned ON and turned OFF with the help of triggering circuit and commutating circuit respectively. It can be turned on or turned off as desired at very high frequency.

During the T_{ON} period, chopper is in ON condition and load voltage is equal to source voltage V_s.

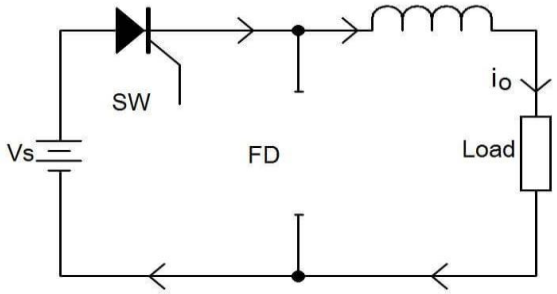

Figure 2.2: Chopper ON condition.

During the T_{OFF} period, chopper is OFF condition, load current flows through the freewheeling diode FD.

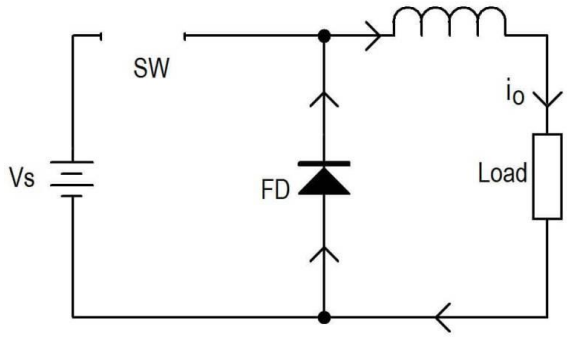

Figure 2.3: Chopper OFF condition.

As a result, load terminals are short circuited by freewheeling diode FD. Thus the load voltage is zero during T_{OFF} period.

In this manner, a chopped DC voltage is produced across the load terminals. The average voltage is given as follows:

$$V_o = \frac{T_{ON}}{T_{ON}+T_{OFF}} V_s = \frac{T_{ON}}{T} V_s = \alpha V_s \quad (2.1)$$

Where:

$\alpha = \frac{T_{ON}}{T}$ Is the duty cycle and $T = T_{ON} + T_{OFF}$.

The above equation shows that, the load voltage is independent of load current and it is clear that the load voltage depends on two factors the supply voltage and the duty cycle of the chopper. Since the supply voltage is constant, load voltage is governed by the duty-cycle of the chopper. In other words, the load voltage is dependent on two factors T_{ON} and T_{OFF}. Hence it is concluded that the average load voltage can be controlled by varying the value of T_{ON} and of T_{OFF} in the following two ways [18]:

1. Varying T_{ON} and keeping the periodic time T constant. This is called constant frequency system.
2. Variable frequency system. i.e., Keeping either T_{ON} constant and varying T_{OFF} or keeping T_{OFF} constant and varying T_{ON}.

2.4 Classification of choppers

Depending upon the direction of the output current and the polarity, the converters can be classified into five classes namely [17]:

- Class A: One-quadrant Operation (1st quadrant only).
- Class B: One-quadrant Operation (2nd quadrant only).
- Class C: Two-quadrant Operation (1, 2 quadrants only).
- Class D: Two-quadrant Operation (1, 4 quadrants only).
- Class E: Four-quadrant Operation (All four quadrants).

2.5 Class E chopper operation

It is a four quadrant chopper (i.e., it operates in all 4 quadrants of the $V_o.i_o$ plane shown in figure 2.4. The load current and load voltage can be both positive and negative. Positive Load Current so that Current flows from source to load and Negative Load Current so that Current flows from load to source. [19]

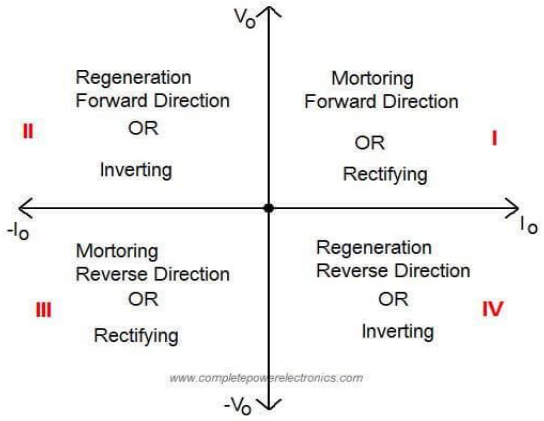

Figure 2.4: $V_o.i_o$ plane.

When the chopper operates in the first and third quadrants, the motor receives energy and the motor operates in the driver mode.

When the motor operation is in second and fourth quadrant power is fed back to the supply and the motor operates in braking mode.

The four quadrant operation of class E chopper system can be achieved by means of two quadrant. Choppers may be connected as shown in figure 2.5. In class E chopper the load is active (i.e., Motor load). The motor's direction of rotation can be reversed without reversing the polarity of its excitation. [19]

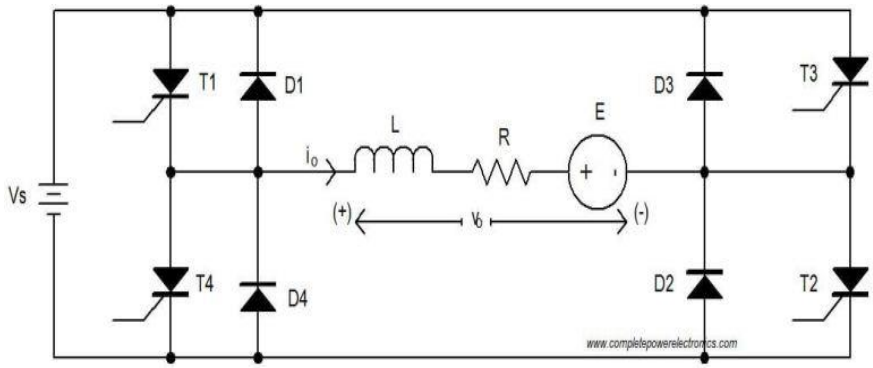

Figure 2.5: A four-quadrant chopper circuit.

In the circuit diagram, T1, T2, D4 and D3 constitute chopper-1 and chopper-2 consists of T4, T3, D1 and D2.

2.5.1 First quadrant operation

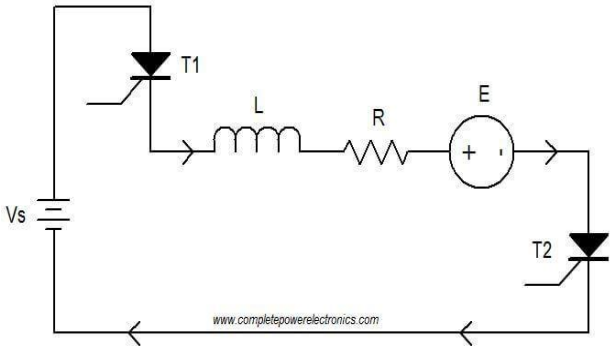

Figure 2.6: First quadrant operation with positive voltage and current in the load.

In first quadrant forward motoring or rectifying operation will happen. Here switch (SCRs) T1 and T2 are turned ON.

Now the voltage across the motor $V_o = V_s =$supply voltage and load current$i_o$starts to flow then both V_o and i_o are in positive direction and the load consumes the power from the source. When SCR T1 is turned OFF, the load current Io freewheels through T2, D4 as shown in figure 2.7. Inductance L stores energy during the time T2 is ON. Thus both V_o and i_o controlled to be in positive and thus in first quadrant. [19]

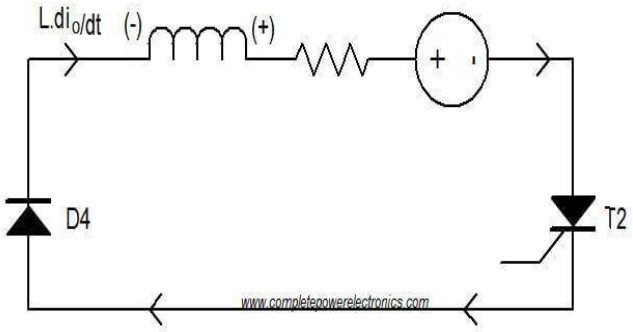

Figure 2.7: first-quadrant operation with zero voltage across the load.

2.5.2 Fourth quadrant operation

When the SCR T2 is turned off, the inductance forces the current through D3 and D4. This current flows through the supply V_s. i.e., the energy is fed back to the supply.

Note that at this moment, the ($V_o = L\frac{di}{dt}$) is more than the supply voltage V_s. Here load voltage is negative but load current is positive leading to the chopper operation in the fourth quadrant. [19]

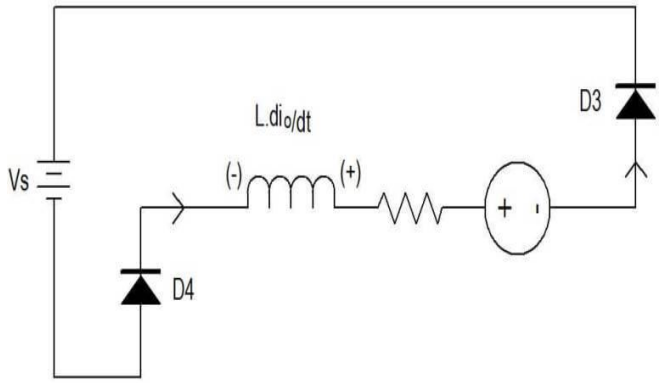

Figure 2.8: fourth–quadrant operation of chopper.

2.5.3 Third quadrant operation

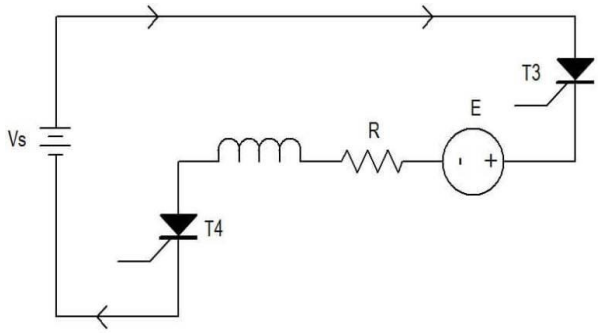

Figure 2.9: Increasing load current mode.

To reverse the direction of rotation of the motor, T3 and T4 are turned ON. Polarity of load voltage V_o reverses and the current flow is also reversed Therefore the operation is in the third quadrant.

Now the T3 is turned OFF, but T4 remains ON.

To maintain the current in the same direction inductance generates voltage and i_o flows in the same direction through D2 and T4 (freewheeling).
With T4 ON reverse current flows through L (Inductance L stores energy during the time T4 is ON), T4, and D2. [19]

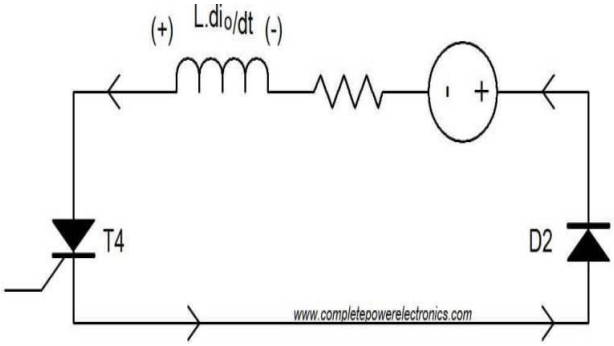

Figure 2.10: Decreasing load current mode.

2.5.4 Second quadrant operation

When T4 is turned OFF, the inductance forces load current through D1 and D2. This current flows through supply. Because ($V_o = L\frac{di}{dt}$) is more than the supply voltage V_s so the energy is fed back to the supply. As load voltage V_o is positive and load current i_o is negative then it is second quadrant operation of chopper. [19]

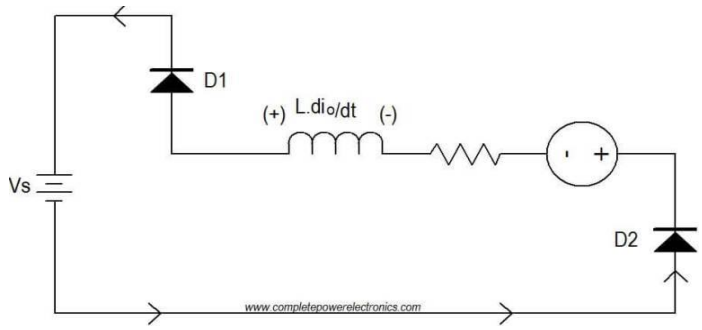

Figure 2.11: Second-quadrant operation with negative.

2.6 Applications of choppers

Choppers are used for DC motor control (battery-supplied vehicles), solar energy conversion, wind energy conversion, electric cars, airplanes and spaceships, where onboard-regulated DC power supplies are required. In general, Chopper circuits are used as power supplies in computers, commercial electronics, and electronic instruments. [17]

Now the motor is said to be in reverse regeneration operation (i.e. regeneration in reverse direction). [17]

III. Open loop and closed loop controller

1. Introduction
2. Open loop structure
3. Closed loop control structure
4. Cascade control structure
5. Performance of a control system
6. Generation of PWM
7. PID controller
8. Controllers design

3.1 Introduction

Motor control is a very old field but interesting development has been done recently by making the use of digital technology for motion control. Sophisticated motor controllers are being used for wide range of application for much complex and accurate motion control.

The function of a DC motor speed controller is to take as an input a signal representing the desired speed and to drive a motor at that speed. The controller may or may not measure the speed of the motor to use it as a feedback for the purpose of error reduction. If it does so, it is called a closed loop system else an open loop system. [1]

3.2 Open loop structure

Open loop system is a type of control system in which uses only the current state as well as its model of the system for computing its output. It is controlled directly, and only, by an input signal, without the benefit of feedback. The basic units of this system are a transducer, an amplifier, a controller and the plant. It starts with a subsystem called an input transducer, and this transducer convert the input signal in the form that can be used by the controller. The amplifier receives a low- level input signal from the transducer and amplifies it enough to drive the plant to perform the desired job.

The distinguishing characteristic of an open-loop system is that it cannot compensate for any disturbances that add to the controller's driving signal (Disturbance 1 in figure 3.1).

Open-loop control systems are not as commonly used as closed-loop control systems because they are less accurate. [7]

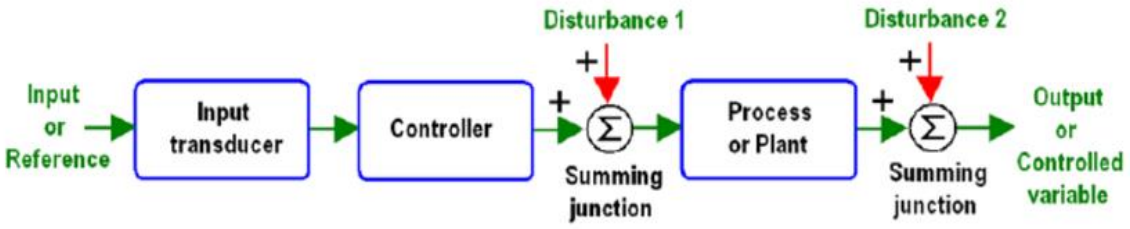

Figure 3.1: Open loop control system.

3.3 Closed loop control structure

A closed-loop control system is one which determines an input forcing function in part by the system response. Then, it compares the measured response of a physical system to the desired response. Actions will be initiated by the difference between the two responses to make the actual response of the system approach the desired response. Hence, the difference signal drives towards zero. Basically closed loop systems use two transducers. One transducer convert the input signal to a form that can be used by the controller and the other one measure the output response of the plant and convert it into a form that can be used by the controller.

These systems measures the output response and then it provides the measurement result through a feedback path to the input where the output is compared with respect to a desired response and this error signal is then used to drive the plant via an actuating signal provided by the controller.

Closed-loop systems, then have the obvious advantage of greater accuracy than open loop systems. They are less sensitive to noise, disturbances and changes in the environment. Transient response and steady-state error can be controlled more conveniently and with greater flexibility in closed-loop systems, often by a simple Adjustment of gain (amplification) in the loop and sometimes by redesigning the controller. [7]

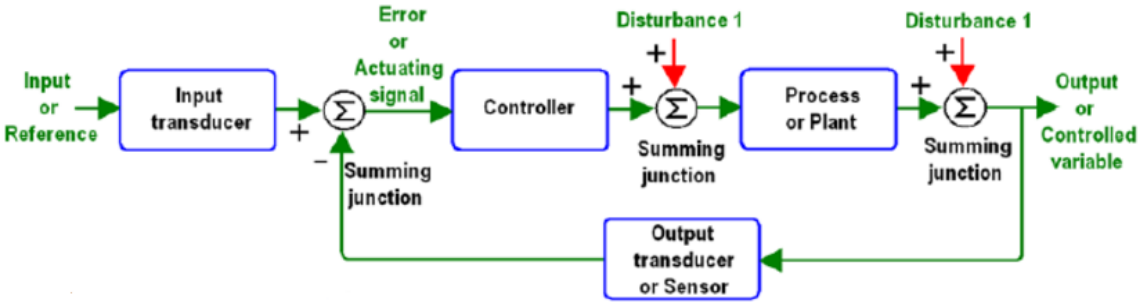

Figure 3.2: Closed loop control system.

3.4 Cascade control structure

A cascade control structure such as that shown in figure 3.3 is used. The cascade control structure is commonly used for motor drives because of its flexibility. It consists of distinct control loops; the innermost current loop and the outer speed loop.

Cascade control requires that the speed of response increases towards the inner loop, with the current loop being the fastest .The cascade control structure is widely used in industry. [3]

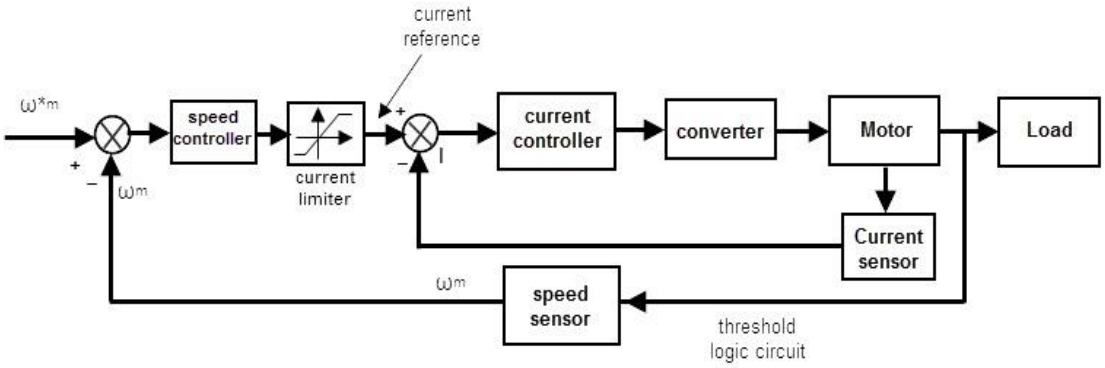

Figure 3.3: Cascade control of motor drive.

3.5 Performance of a control system

It describes how well the output tracks a change in the reference input. Frequently, the performance characteristics of a control system are specified in terms of the transient response to a unit-step input, since it is easy to generate and is sufficiently drastic (If the response to a step input is known, it is mathematically possible to compute the response to any input).

In specifying the transient-response characteristics of a control system to a unit-step input, it is common to specify the following and are shown graphically in figure 3.4:

1. Delay time, t_d: The delay time is the time required for the response to reach half the final value the very first time.

2. Rise time, t_r: The rise time is the time required for the response to rise from 10% to 90%, 5% to 95%, or 0% to 100% of its final value. For underdamped second order systems, the 0%to 100% rise time is normally used.

3. Peak time, t_p: The peak time is the time required for the response to reach the first peak of the overshoot.

4. Maximum (percent) overshoot, M_p: The maximum overshoot is the maximum peak value of the response curve measured from unity. If the final steady-state value of the response differs from unity, then it is common to use the maximum percent overshoot, The amount of the maximum (percent) overshoot directly indicates the relative stability of the system.

5. Settling time, t_s: The settling time is the time required for the response curve to reach and stay within a range about the final value of size specified by absolute percentage of the final value (2%or 5%). The settling time is related to the largest time constant of the control system which percentage error criterion to use may be determined from the objectives of the system design.

The time-domain specifications just given are quite important, since most control systems are time domain systems; that is, they must exhibit acceptable time responses. (This means that, the control system must be modified until the transient response is satisfactory). [4]

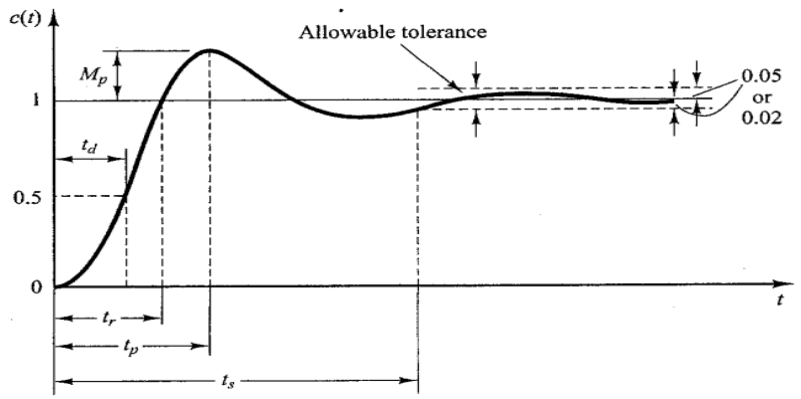

Figure 3.4: Unit step response curve showing t_d, t_p, t_r, M_p and t_s.

3.6 Generation of PWM

PWM technique is widely used in many applications where we want to feed our system in pulses, it is used in the control of the speed of a dc motor by varying the average voltage fed to it, this is done through varying the duty cycle of the signal over the full range.

The term duty cycle describes the proportion of on time to the period of signal. Duty cycle is expressed in percent:

$$Duty\ cycle = \frac{ON\ TIME}{PERIOD} * 100\% \quad (3.1)$$

There is a carrier signal and a modulating signal, these two signals are compared using comparator, when the saw tooth voltage (triangle) rises above the reference voltage the output is high so the switch is turned on. However, if it is below the reference voltage the output will be zero hence the switch will be turned off, as in Figure 3.5. [8]

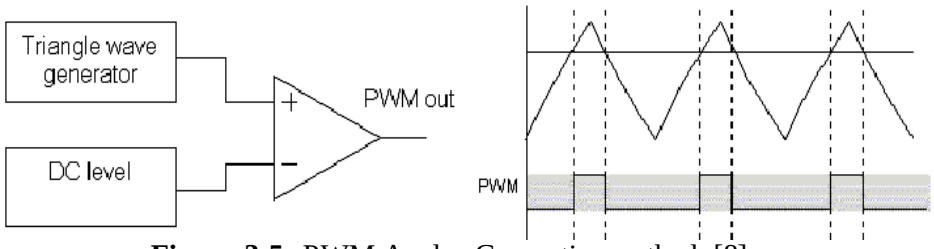

Figure 3.5: PWM Analog Generation method. [8]

3.7 PID Controller

A PID Controller algorithm involves a parallel combination of proportional integral and derivative control. The Proportional term determines how the controller responds to an existing error, the Integral term determines the response based upon sum of recent errors and finally derivative term determines the response of the controller, based on the rate of change of the error. The weighted sum of all the actions is then used to adjust the process via a final controlling element such as PWM Generator. [8]

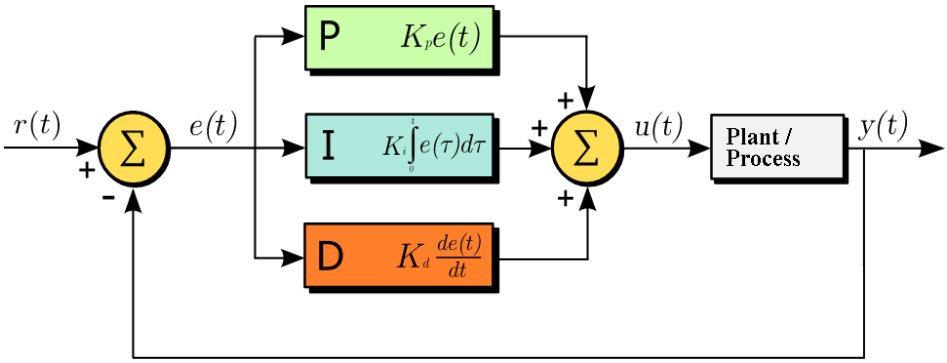

Figure 3.6: Block diagram of PID controller. [8]

3.7.1 Proportional term

The proportional gain changes the output in such a way that the change is proportional to the existing error. The proportional term is given by [8]:

$$p_{out} = K_p e(t) \tag{3.2}$$

Where:

p_{out} : Proportional output.

K_p: Proportional gain, a tuning parameter.

e(t): Error= SP-PV(t) is the error (SP is the set-point, and PV(t) is the process variable).

t : the time or instantaneous time (the present).

3.7.2 Integral term

The integral term makes a change to the output that is proportional to both the error magnitude and the error duration; the error is accumulated over the time and this error is then multiplied by a constant known as integral gain and then it is added to the controller output; the integral term is given by:

$$I_{out} = K_i \int_0^t e(\tau)d\tau \tag{3.3}$$

Where:

I_{out} : Integral output.

K_i: Integral gain, a tuning parameter.

$e(\tau)$: The Error.

t: Time or instantaneous time.

τ: The variable of integration (takes on values from time 0 to the present t).

The integral term reduces or even completely eliminates the steady state error and reduces the response time for a change in error but it can cause the output of the controller to overshoot the set point value. [8]

3.7.3 Derivative term

The derivative term is calculated by determining the slope of the error with respect to time and multiplying the derivative gain K_d with the rate of change of error.

The derivative term is given by:

$$D_{out} = K_d \frac{d}{dt} e(t) \tag{3.4}$$

Where:

D_{out} : Derivative term of output.

K_d : Derivative gain, a tuning parameter.

e(t): Error= SP-PV(t) is the error (SP is the set-point, and PV(t) is the process variable).

t: Time or instantaneous time.

To calculate the output of the PID Controller the proportional, integral and derivative terms are summed together. [8]

Let u(t) be the controller output, then the final form of the PID algorithm is:

$$pid_{out} = K_p e(t) + K_i \int_0^t e(\tau) d\tau + K_d \frac{d}{dt} e(t) \tag{3.5}$$

3.8 Controllers design

The overall closed-loop system of DC motor drive is shown in figure 3.7, the design of control loops starts from the innermost (fastest) loop to the outer (slowest) loop. The reason to proceed from the inner to the outer loop in the design process is that the gain and time constants of only one controller at a time are solved, instead of solving for the gain and time constants of all controllers simultaneously. [2]

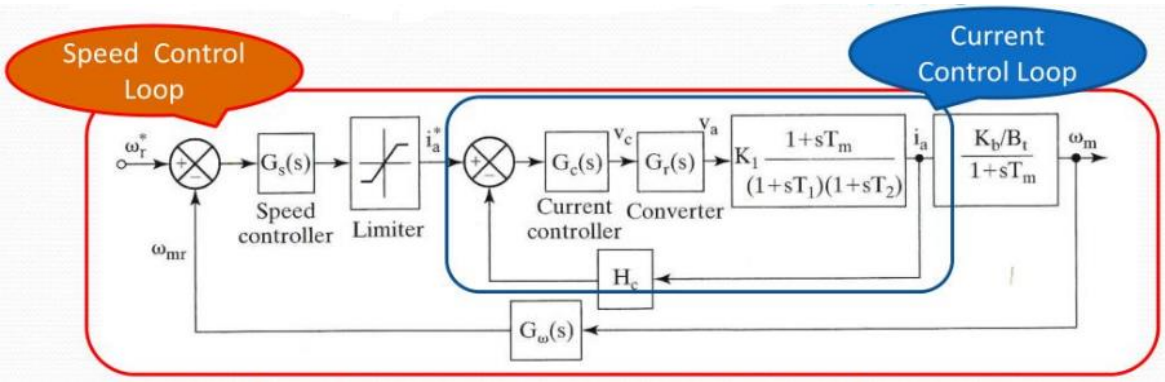

Figure 3.7: Block diagram of the DC motor drive. [20]

In some applications such as traction application, the motor drive need not be speed controlled but may be torque controlled. In that case, the current loop is essential and exists regardless of whether the speed control loop is going to be closed. The performance of the outer loop is dependent on the inner loop; therefore, the tuning of the inner loop has to precede the design and tuning of the outer loop. [2]

Current and speed controllers

The current control loop: it is shown in figure 3.8.

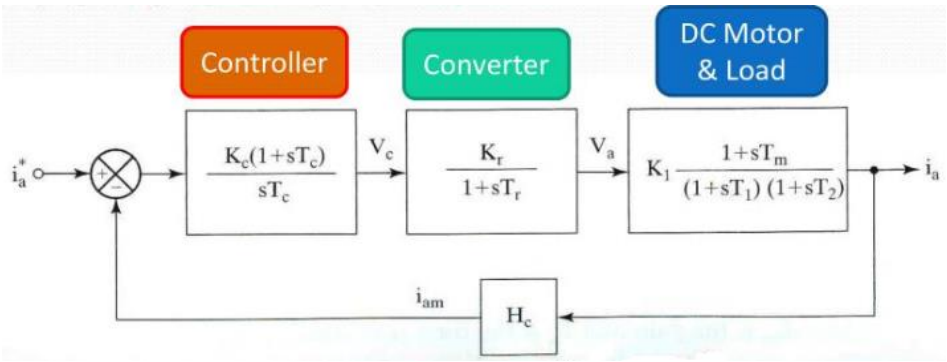

Figure 3.8: Current-control loop. [20]

The open loop gain transfer function is,

$$GH_{ol}(s) = \left\{\frac{K_1 K_c K_r H_c}{T_c}\right\} \frac{(1+sT_c)(1+sT_m)}{s(1+sT_1)(1+sT_2)(1+sT_r)} \quad (3.6)$$

Where:

T_1, T_2 : Electrical time constant of the motor.

K_1 : Motor gain.

B_t : Total friction co-efficient in N-M/(rad/sec).

J : Moment of inertia.

K_c : Current controller gain.

T_c : Current controller time constant.

K_r : Converter gain.

T_r : Converter delay time.

From the open loop gain, the system is 4th order (due to 4 poles of the system) then if designing without computers, simplification is needed.

T_m Is in order of one second and in the vicinity of the gain crossover frequency, we see that the following approximation is valid:

$$(1 + sT_m) \cong sT_m \tag{3.7}$$

And by making

$$T_c = T_2 \tag{3.8}$$

Then the final open loop gain function:

$$GH_{ol}(s) \cong \frac{K}{(1+sT_1)(1+sT_r)} \tag{3.9}$$

Where

$$K = \frac{K_1 K_c K_r H_c T_m}{T_c} \tag{3.10}$$

The system is now of 2nd order and from the closed loop transfer function:

$$G_{cl}(s) = \frac{GH_{ol}(s)}{1+GH_{ol}(s)} \tag{3.11}$$

The closed loop characteristic equation is:

$$(1 + sT_1)(1 + sT_r) + k \tag{3.12}$$

By comparing the system characteristic equation with the standard 2nd order system equation:

$$s^2 + 2\zeta\omega_n + \omega_n^2 \tag{3.13}$$

So that we can easily design the current controller. [2][20]

The speed control loop:

To design the speed loop, the 2nd order model of current loop must be replaced with an approximate 1st order model to reduce the order of the overall speed loop gain function by adding T_t to T_1:

$$T_3 = T_r + T_1 \tag{3.14}$$

Then

$$\frac{I_a(s)}{I_a^*(s)} = \frac{\frac{K_c K_1 K_r T_m}{T_c(1+sT_3)}}{1+\frac{K_c K_r K_1 H_c T_m}{T_c(1+sT_3)}} = \frac{K_i}{(1+sT_i)} \tag{3.15}$$

Where:

$$T_i = \frac{T_3}{1+K_{fi}} \tag{3.16}$$

$$K_i = \frac{K_{fi}}{H_c(1+K_{fi})} \tag{3.17}$$

$$K_{fi} = \frac{K_1 K_c K_r H_c T_m}{T_c} \tag{3.18}$$

1st order approximation of current loop used in speed loop design.

If more accurate speed controller design is required, values of K_i and T_i should be obtained experimentally.

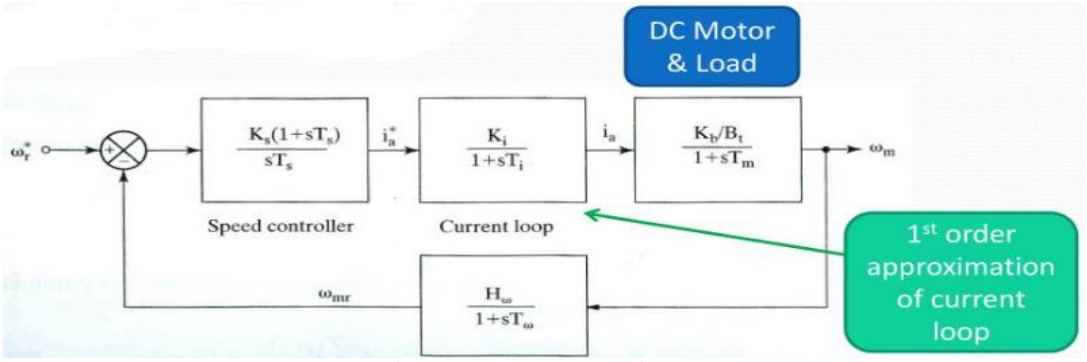

FIGURE 3.9: Simplified block diagram of the DC motor drive. [20]

Assume there is a unity feedback:

$$G_\omega(s) = \frac{H_\omega}{(1+sT_\omega)} = 1 \tag{3.19}$$

The open loop gain function will be:

$$GH(s) = \left\{\frac{K_B K_S K_i}{B_t T_s}\right\} \frac{(1+sT_s)}{s(1+sT_i)(1+sT_m)} \tag{3.20}$$

From the open loop gain, the system is of 3rd order. Again If designing without computers, simplification is needed.

Relationship between the denominator time constants in the previous equation:

$$T_i < T_m \tag{3.21}$$

Hence, design the speed controller such that:

$$T_s = T_m \tag{3.22}$$

After simplification, open loop gain function:

$$GH(s) \cong \frac{K_\omega}{s(1+sT_i)} \tag{3.23}$$

Where:

$$K_\omega = \frac{K_B K_s K_i}{B_t T_s} \tag{3.24}$$

The controller is now of 2nd order.

Again from the closed loop transfer function, the characteristic equation is:

$$s(1 + sT_i) + K_\omega \tag{3.24}$$

By comparing the system characteristic equation with the standard 2nd order system equation (3.13), we can easily design the speed controller. [2][20]

IV. System parameters identification

4.1 Introduction

After implementing the whole system and acquiring the required signals, it can be noticed that the stage of parameters identification of dc motor as well the controller is necessary. The DC motor parameters needed to be identified are:

K_g: Tacho-Generator constant.

L_a : The inductance of the DC motor.

R_a: The armature resistance of the DC motor.

K_v: Motor voltage constant.

K_t: The Motor torque constant. Since the manufacturer's data sheet.is not available, it is required to measure these constants experimentally.

4.2 DC motor parameters identification tests

The setup that we are going to use is shown in figure 4.1.

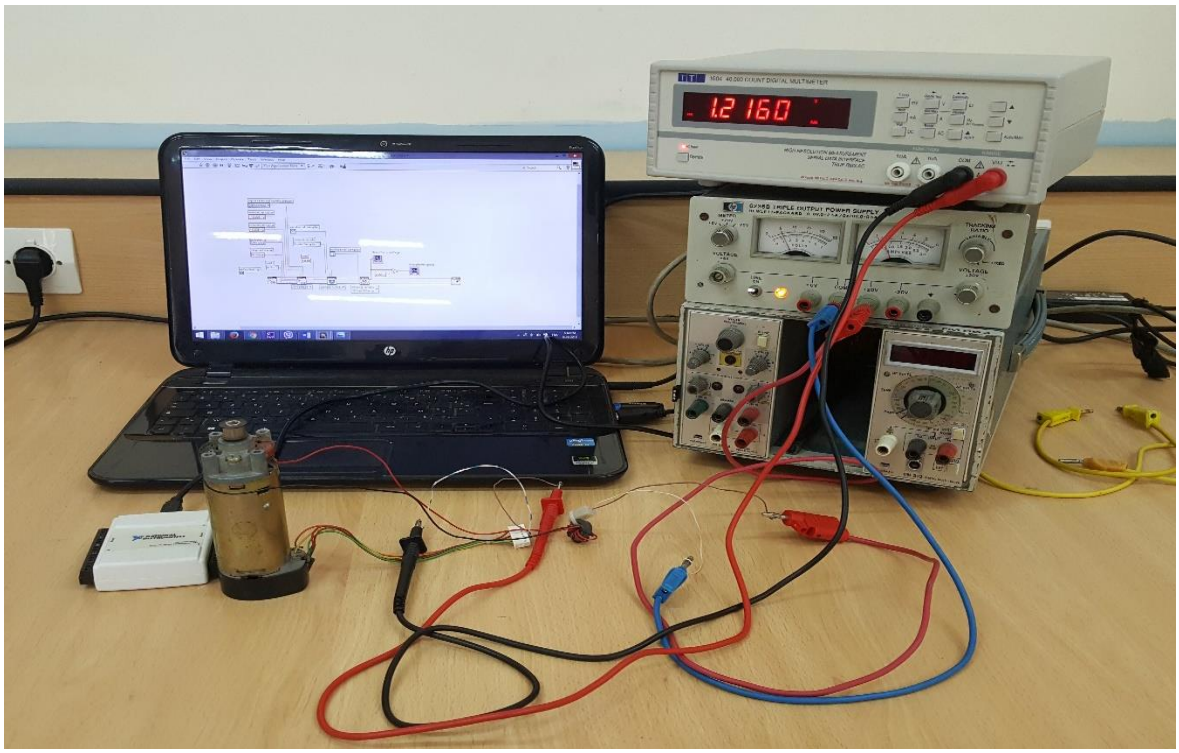

Figure 4.1: Setup used for identifying the motor parameters.

The data are repeated 3 times for more accurate results and given in Table 4.1.

Table 4.1: the experimental data of the DC motor.

V_a(V)	I_a(A)	W(rpm)	V_g(V)	V_a(V)	I_a(A)	W(rpm)	V_g(V)	V_a(V)	I_a(A)	W(rpm)	V_g(V)
1.05	0.144	96	0.128	1.05	0.145	80	0.140	1.05	0.147	108	0.149
2	0.145	300	0.375	2	0.156	288	0.362	2	0.155	312	0.376
3	0.158	516	0.631	3	0.169	497	0.625	3	0.168	518	0.640
4	0.164	798	0.909	4	0.176	810	0.892	4	0.168	802	0.902
5	0.170	1044	1.187	5	0.176	1070	1.203	5	0.178	1052	1.191
6	0.174	1300	1.478	6	0.177	1328	1.500	6	0.180	1286	1.492
7	0.176	1650	1.768	7	0.180	1710	1.778	7	0.180	1680	1.790
8	0.176	1860	2.058	8	0.181	1880	2.080	8	0.181	1876	2.100
9	0.177	2070	2.345	9	0.182	2055	2.360	9	0.182	2080	2.320
10	0.178	2288	2.635	10	0.183	2300	2.650	10	0.182	2345	2.689
11	0.179	2310	2.928	11	0.183	2415	2.943	11	0.184	2450	3.057
12	0.182	2390	3.231	12	0.184	2495	3.105	12	0.184	2518	3.162

4.2.1 Tacho-Generator constant (K_g)

Using equation (4.1) and the data of the graph shown in figure (4.2), the tacho-generator constant Kg may be obtained,

$$V_g = K_g W_m \tag{4.1}$$

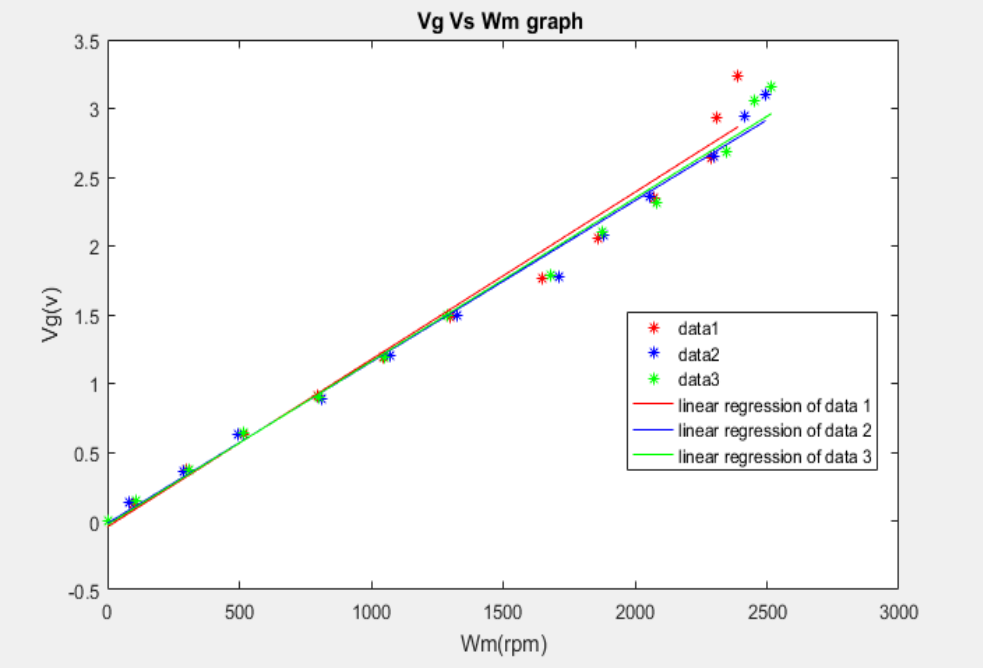

Figure 4.2: plot of the speed (rpm) vs. the tacho-voltage (v).

The Tacho-generator constant is represented by the slope of the graph in figure 4.3, by using the linear regression of the 3 repeated sets of data obtained and then taking the average value, we get:

$$K_g = 0.0012\ V/rpm \tag{4.2}$$

Or

$$K_g = 0.01146 \frac{V}{rad/sec} \tag{4.3}$$

4.2.2 Motor voltage constant (K_v)

We have:

$$E_c = K_v W_m \tag{4.4}$$

And at steady state conditions:

$$V_a = R_a I_a + E_c \tag{4.5}$$

Then

$$V_a = R_a I_a + K_b W_m \tag{4.6}$$

$$\frac{V_a}{I_a} = K_v \frac{W_m}{I_a} + R_a \tag{4.7}$$

To obtain K_v we must plot $\frac{V_a}{I_a}$ versus $\frac{W_m}{I_a}$.

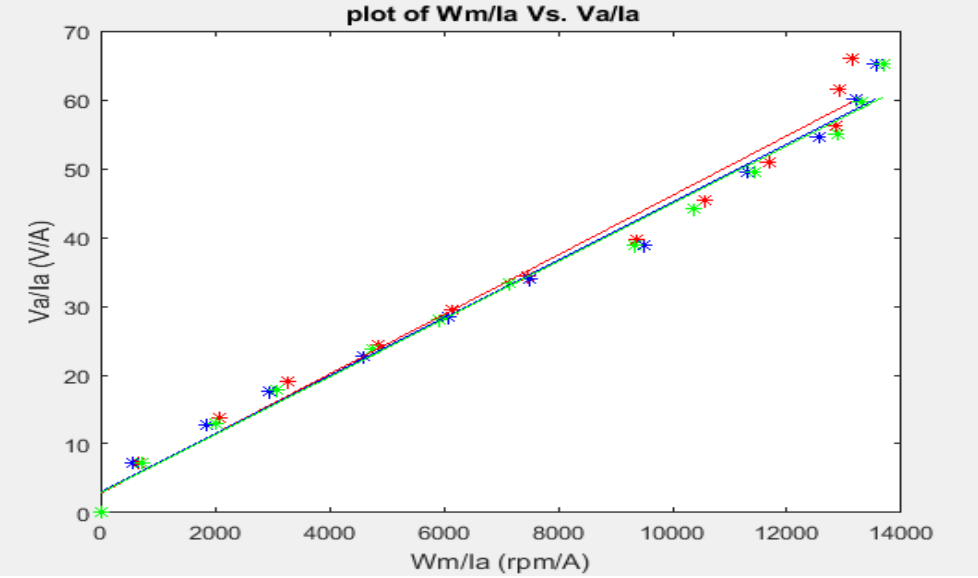

Figure 4.3: plot of $\frac{V_a}{I_a}$ vs $\frac{W_m}{I_a}$.

Using the same procedure as before the back EMF constant is:

$$K_v = 0.0042\ V/rpm \tag{4.8}$$

4.2.3 The armature resistance (R_a)

By applying directly the multi-meter on the dc motor terminals we can measure:

$$R_a = 8.6\ \Omega \tag{4.9}$$

4.2.4 The armature inductance (L_a)

By applying an AC voltage with $V_{MAX} = 0.6V$.

Then $V_{RMS} = 0.424V$; $f = 50Hz$; $I = 12.3\ mA$

Now we have

$$Z = \frac{V_{rms}}{I_{rms}} \tag{4.10}$$

$$Z = \sqrt{2\pi F^2 + R_a^2} \tag{4.11}$$

$$Z = \sqrt{x_l^2 + R_a^2} \tag{4.12}$$

So

$$x_l = \sqrt{Z^2 - R_a^2} = \sqrt{(\frac{V_{rms}}{I_{rms}})^2 - R_a^2} = \sqrt{(\frac{0.424}{0.0087})^2 - 8.6^2} = 47.97 \tag{4.13}$$

Finally $$L_a = \frac{X_l}{2\pi F} = \frac{47.97}{2\pi * 50} = 0.153\ \text{H} \tag{4.14}$$

4.2.5 The motor torque constant (K_t)

Since $K_t = K_v$, so:

$$K_t = 0.0042\ V/rpm \tag{4.15}$$

4.2.6 Motor transfer function T(s)

The DC motor transfer function is a first order with the form:

$$T(s) = \frac{1/R_a}{1+\tau s} \tag{4.16}$$

Using The DAQ to acquire the analog signal which is the output of the tachometer.

So for input voltage 4V we obtain the voltage response graph:

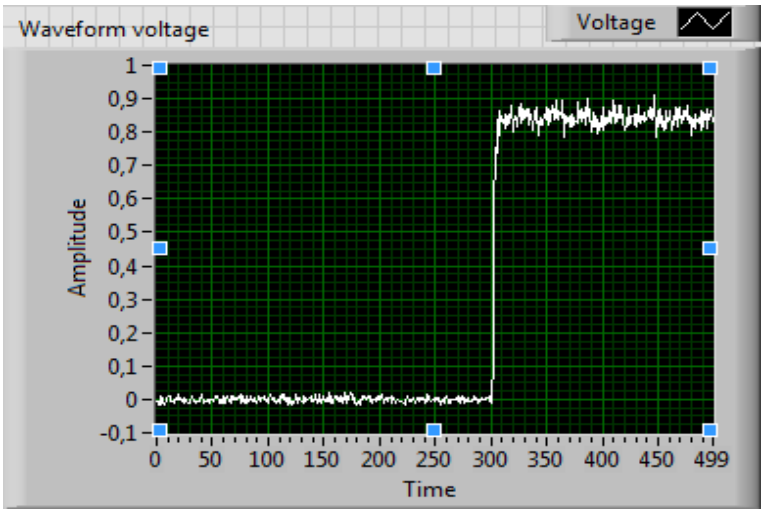

Figure 4.4: Tacho-voltage waveform with 4V input voltage using LABVIEW.

Using LABVIEW, we can export our data to excel so:

Amplitude = 0.90V → 0.63*0.90= 0.567V.

Time at 0.567V is 303 so

$$t_1 = 303 - 300 = 3$$

$$K_1 = \frac{V_{out}}{V_{in}} = \frac{0.9}{4} = 0.225 \qquad (4.17)$$

For input voltage 8V, we obtain the voltage response graph as illustrated in Fig.4.5.

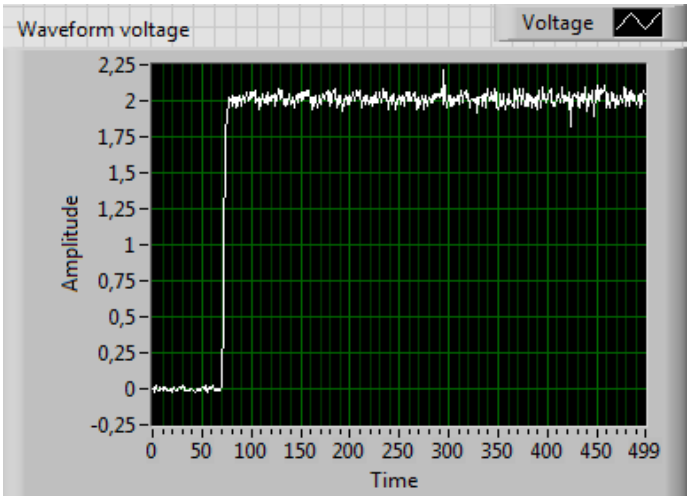

Figure 4.5: Tacho-voltage waveform with 8V input voltage using LABVIEW.

Using LABVIEW we can export our data to excel so:

Amplitude = 2.08V → 0.63*2.08= 1.310V.

Time at 1.310V is 72.5 so

$$t_2 = 72.5 - 70 = 2.5$$

$$K_2 = \frac{V_{out}}{V_{in}} = \frac{2.08}{8} = 0.260 \quad (4.18)$$

For input voltage 12V, we obtain the voltage response graph as illustrated in Fig.4.6.

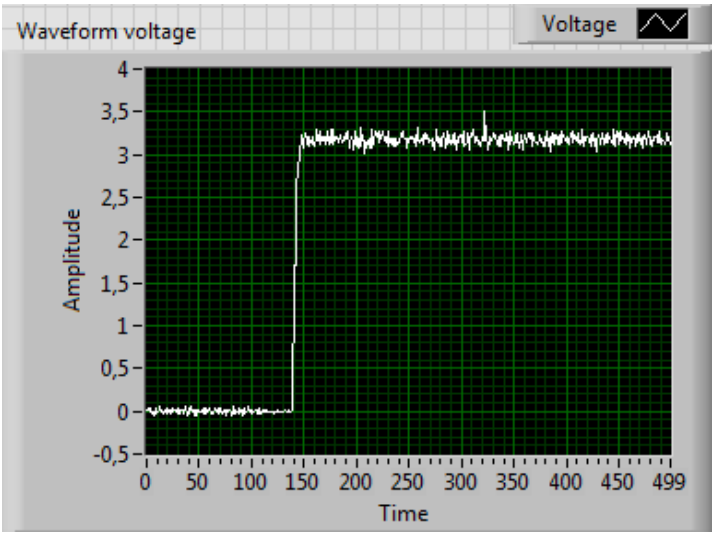

Figure 4.6: Tacho-voltage waveform with 12V input voltage using LABVIEW.

Using LABVIEW we can export our data to excel so:

Amplitude = 3.166V → 0.63*3.166= 1.995V.

Time at 1.995 V is 142.3 so

$$t_3 = 142.3 - 140 = 2.3$$

$$K_3 = \frac{V_{out}}{V_{in}} = \frac{3.166}{12} = 0.264 \quad (4.19)$$

So the average time constant is:

$$t_{avg} = \frac{t_1 + t_2 + t_3}{3} = \frac{3 + 2.5 + 2.3}{3} = 2.6 \quad (4.20)$$

Since the sampling rate used in Labview is 50 Hz which means 0.02s, then:

$$T_{avg} = t_{avg} * 0.02 = 2.6 * 0.02 = 0.052\ s \quad (4.21)$$

And the average coefficient K is:

$$K = \frac{K_1 + K_2 + K_3}{3} = \frac{0.225 + 0.260 + 0.264}{3} = 0.250 \quad (4.22)$$

Then the transfer function will be:

$$T(s) = \frac{0.250}{1+0.052\ s} \tag{4.23}$$

4.2.7 Motor inertia (J_m)

Motor rotor inertia can be measured as follow:

$$\text{Inertia [kg. m2]} = \frac{\text{acceleration torque [A.rad/s^2]}}{\text{acceleration [rad /s^2]}} \tag{4.24}$$

To do this test it is necessary to measure the acceleration of the motor rotor and the acceleration torque of the motor rotor. These two parameters are described as follows:
1. *Acceleration*: This parameter is determined by putting a step in voltage into the motor winding to bring the motor up to rated speed. The motor will accelerate exponentially. The acceleration is a measure of the rate of change of velocity over a period of time. The acceleration is therefore the change in velocity for the linear part of the exponential curve divided by the time elapsed for the detected rate of change in velocity.

2. *Torque*: When the step in input voltage is applied to the motor input, the maximum value of current should be noted. This current must be converted to torque. The torque is equal to

$$\text{Torque [N.m]} = \text{amps [A]* KT [(N*m)/A]} \tag{4.25}$$

For input voltage 12V, the graph as shown in figure 4.5

The acceleration is

$$\alpha = \frac{2.97897-0.012028}{(145-143)*0.02} * 0.01146 = 0.85\ rad/s^2 \tag{4.26}$$

The acceleration torque is

$$\alpha_T = 0.184\ A * 0.0401\left(N.\frac{m}{A}\right) = 0.007378\ N.m \tag{4.27}$$

The inertia is

$$J = \frac{0.007378}{0.85} = 0.00868\ Kg.m^2 \tag{4.28}$$

4.3 PID Controller Parameters Identification

The permanent magnet dc motor supplied by a switch-mode PWM dc-dc converter is used in this experimental test. The DC motor parameters as given in table 4.2 are used in this test. The speed controller type is PID:

Table 4.2: The DC motors parameters.

System parameters	value
R_a	8.6 $\boldsymbol{\Omega}$
L_a	0.153 H
J_{ma}	0.00868 $Kg.m^2$
B	0
K_t	0.0042 V/rpm
K_v	0.0042 V/rpm
K_g	0.01146 V/(rad/s)

The whole system with the obtained parameters have been implemented using MATLAB, where the PI controller parameters are tuned as illustrated in Figs.4.7 & 4.8 and given in Table 4.3.

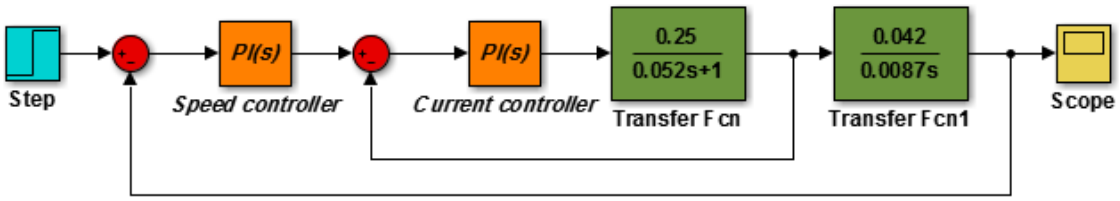

Figure 4.7: The Simulink model of the system simulated in MATLAB.

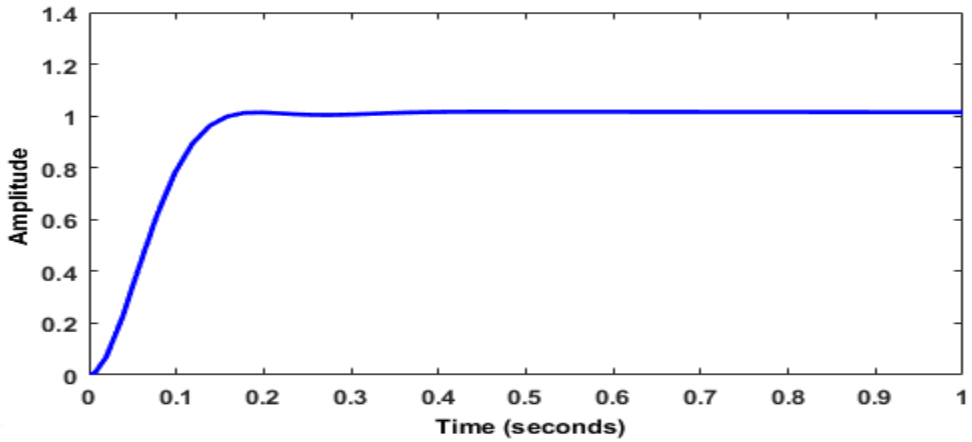

Figure 4.8: Step response system simulated in MATLAB.

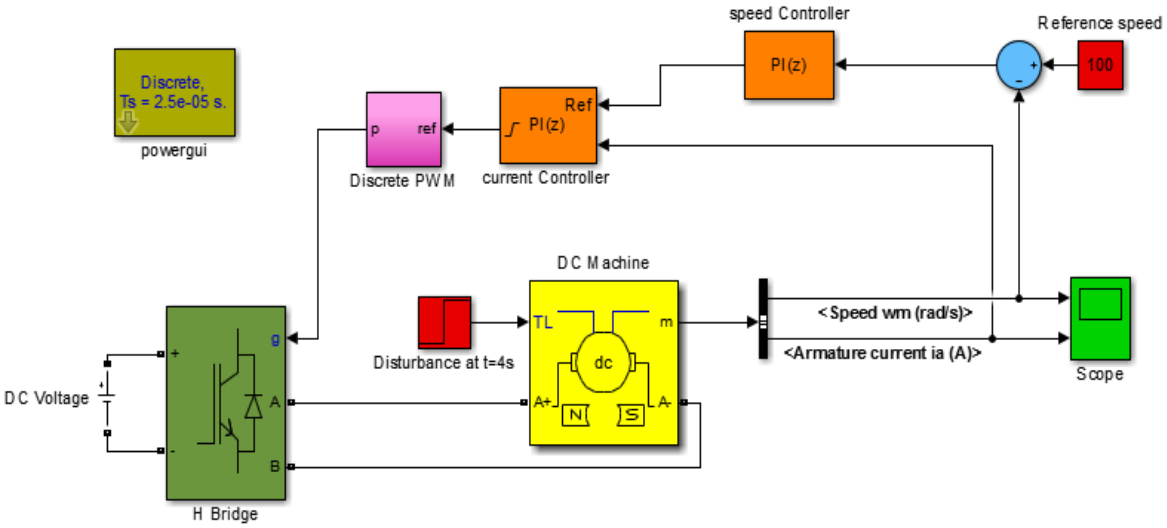

Figure 4.9: Simulation of the whole system in MATLAB.

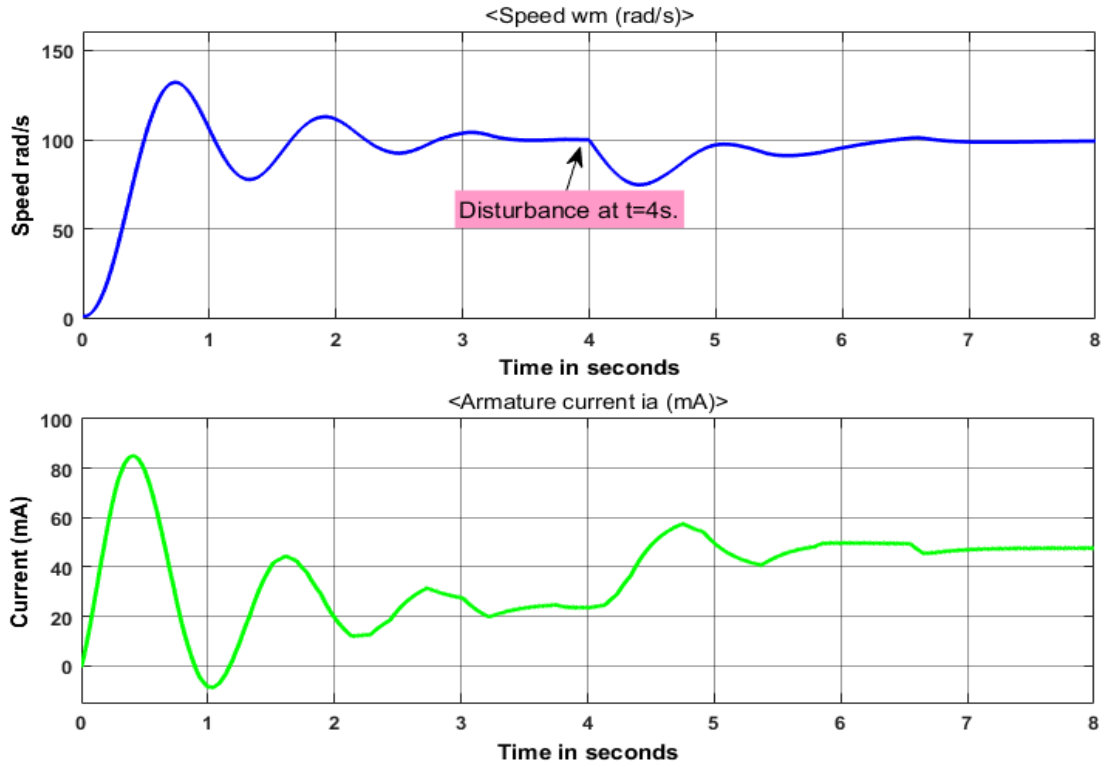

Figure 4.10: The system response simulated in MATLAB.

Table 4.3: PI controller parameters.

Parameters	Value (speed controller)	Value (current controller)
K_p	7.127	0.0016623
K_i	8.135	0.0223009

V. Implementation of LABVIEW based controller

1. Introduction
2. DC motor interfacing with DAQ card: IC L293D
3. PID controller parameters identification
4. Results and discussion

5.1 Introduction

Motor control is a very old field but interesting development has been done recently by making the use of digital technology for motion control. Sophisticated motor controllers are being used for wide range of application for much complex and accurate motion control. However development time and the cost factor have increased due to error in design and integration which can be detected only when the code is run on the actual hardware.

5.2 DC motor interfacing with DAQ card: IC L293D

L293D is a quadruple high current half-H driver for the DC motor, The L293D is designed to provide bidirectional drive currents of up to 600mA at voltages from 4.5 V TO 36 V. All the inputs are TTL compatible. Drivers are enabled in pairs, with drivers 1 and 2 enabled by 1,2EN and drivers 3 and 4 enabled by 3,4EN. L293D is used to drive the motor. Basically the output of the PWM Generator is given to the EN1 pin of the L293D.

When the PWM Generator output is high it enables the driver. 1A and 2A are two inputs; 1Y and 2Y are the outputs. The output terminal of the L293D is connected to the dc motor input. When 1A is high and 2A is low the motor will rotate in counter clock-wise direction and when the polarity is reversed then the motor will rotate in clockwise direction.

The pin and the block diagram of L293D IC are shown below:

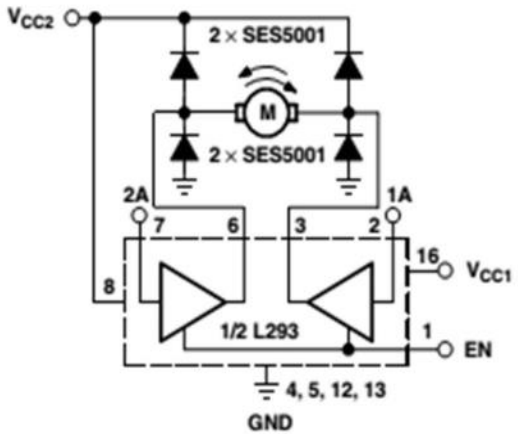

EN	1A	2A	FUNCTION
H	L	H	Turn right
H	H	L	Turn left
H	L	L	Fast motor stop
H	H	H	Fast motor stop
L	X	X	Fast motor stop

L = low, H = high, X = don't care

Figure 5. 1: The block diagram of L293D IC and its function table.

5.3 Experimental setup

5.3.1 DC motor hardware setup

The DC motor is driven by the driver IC L293D. The following figure shows the schematic diagram of the DC motor with IC L293D:

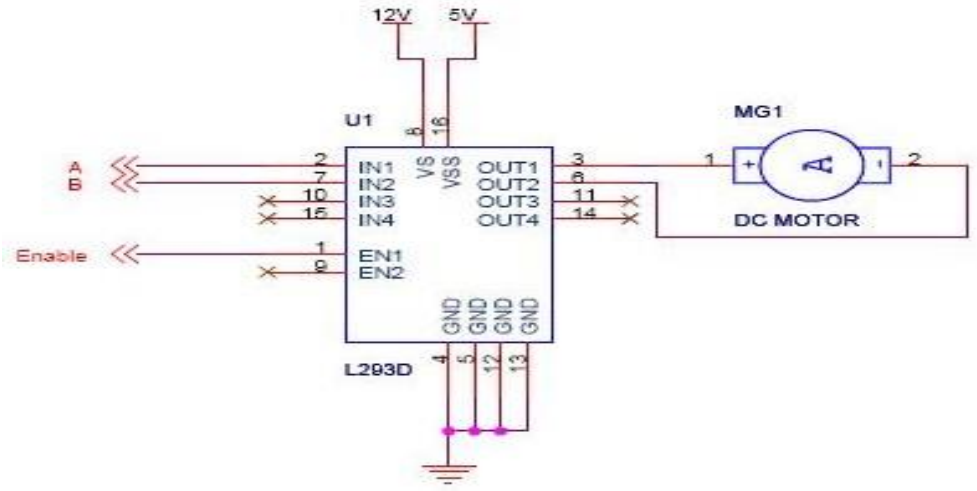

Truth Table

A	B	Description
0	0	Motor stops or Breaks
0	1	Motor Runs Anti-Cloclwise
1	0	Motor Runs Clockwise
1	1	Motor Stops or Breaks

Figure 5. 2: schematic for showing the interfacing of the DC motor with L293D.

From the circuit we can see that the motor in connected at terminals 3 and 6 and terminals 1.2 and 7 i.e. Enable, A and B are used to control the motor. The output of the PWM generator is fed to the Enable input and inputs A and B controls the direction of running of the DC motor such that A is low and B is high and the motor turns left in our case.

5.3.2 The current sensing circuit

The armature current 'I_a' must be converted into a voltage before used as a feedback signal, a differential amplifier have been used to perform this conversion. This is illustrated in Fig 5.3. Where:

$$V_{out} = \frac{R_1}{R_2} * R_5 * \left(1 + \frac{R_8}{R_9}\right) = 30I_a \qquad (5.1)$$

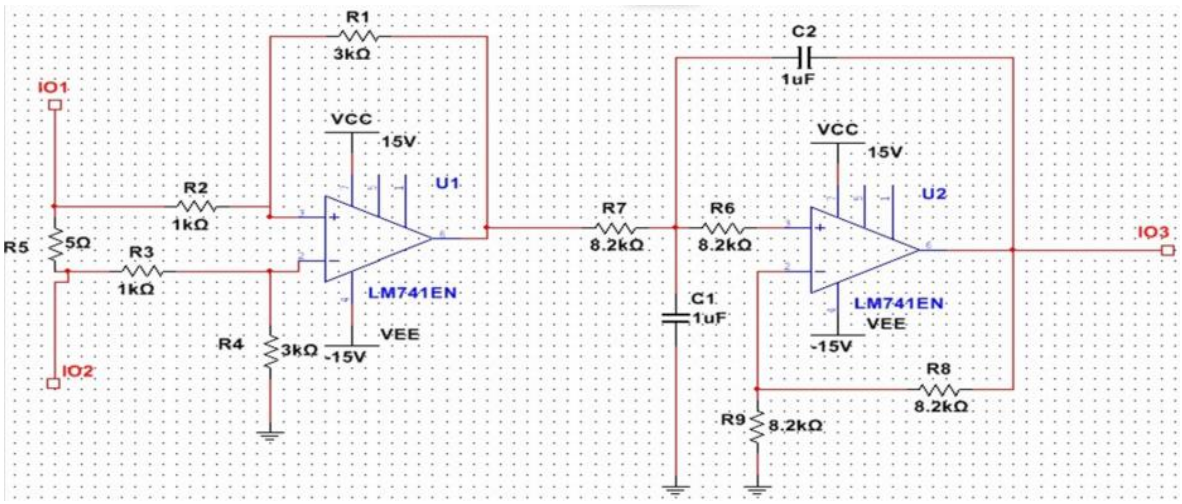

Figure 5. 3: Differential amplifier and second order filter circuit for interfacing the current.

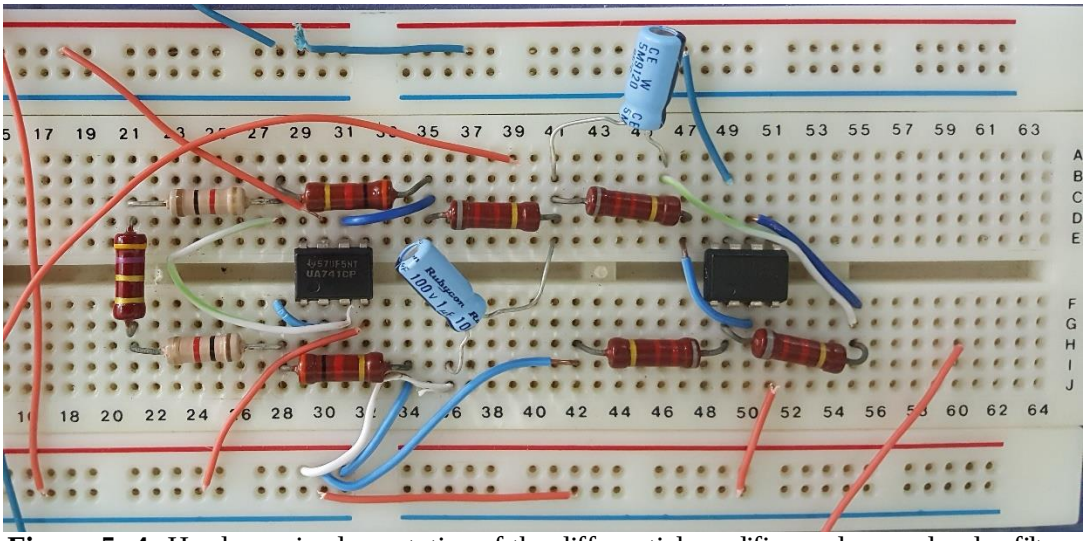

Figure 5. 4: Hardware implementation of the differential amplifier and second order filter.

5.3.3 The Filter circuit Design Procedure

The speed of the motor is obtained by a Tacho-generator; the interfacing circuit for the output of the Tacho-voltage is shown in figure 5.5 Where:

$$V_{out} = V_g * \left(1 + \frac{R_8}{R_9}\right) = 2V_g \qquad (5.2)$$

The feedback signals are connected to DAQ NI USB-6009, which, after that can be used to perform the PID-speed controller.

To design the filter for the Tacho-voltage to be compatible with the DAQ in range of 0 to 10 v and also to minimize the ripple we set:

$$R_6 = R_7 = R_8 = R_9 = 8.2K\Omega \quad \text{And} \quad C_1 = C_2 = 1\mu F$$

So

$$F_{cut-off} = \frac{1}{2\pi RC} = 20Hz \tag{5.3}$$

And the gain

$$A = 1 + \frac{R_8}{R_9} = 2 \tag{5.4}$$

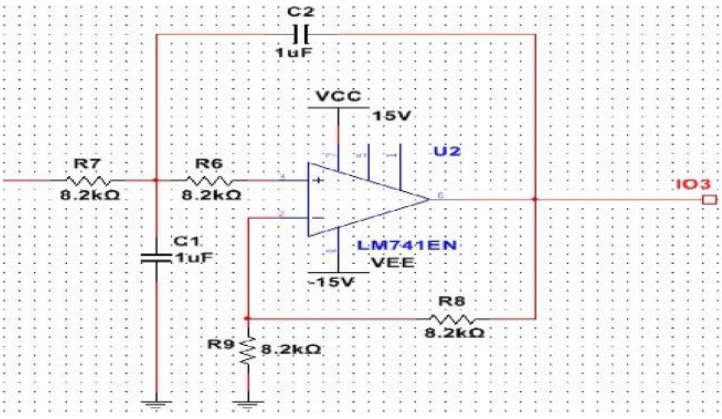

Figure 5.5: Second order filter circuit for interfacing the current.

5.3.4 The PWM circuit Design Procedure

The output of the NI USB-6009 is fed to the PWM circuit as shown in figure 5.6.

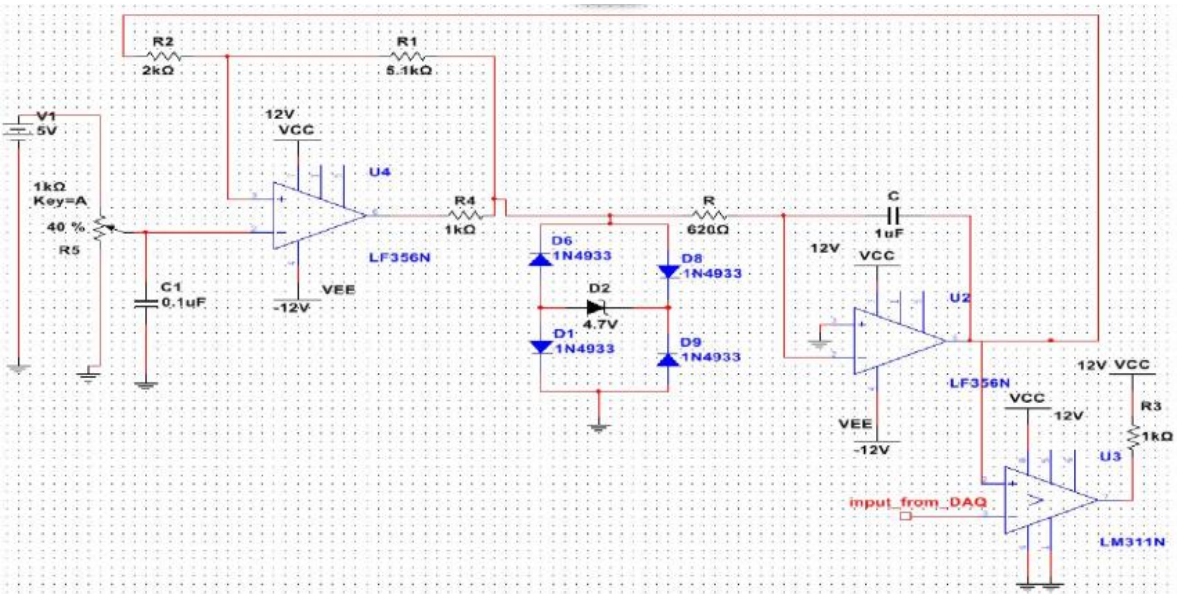

Figure 5. 6: Schematic diagram of the PWM circuit used.

We have:

$$V_o = V_z + 2V_d \tag{5.5}$$

$$V_a = \left(1 + \frac{R_2}{R_1}\right) V_{ref} + \frac{R_2}{R_1} V_o \tag{5.6}$$

$$V_b = \left(1 + \frac{R_2}{R_1}\right) V_{ref} - \frac{R_2}{R_1} V_o \tag{5.7}$$

And the relations:

$$F = \frac{1}{4\frac{R_2}{R_1}RC} \tag{5.8}$$

$$V_b - V_a = V_{peak-to-peak} \tag{5.9}$$

In this PWM circuit the zener diode that have been used have 4.7 V and the 1N4002 diode have a 0.7 V, hence:

$$V_o = 4.7 + 2 * (0.7) = 6.1V \tag{5.10}$$

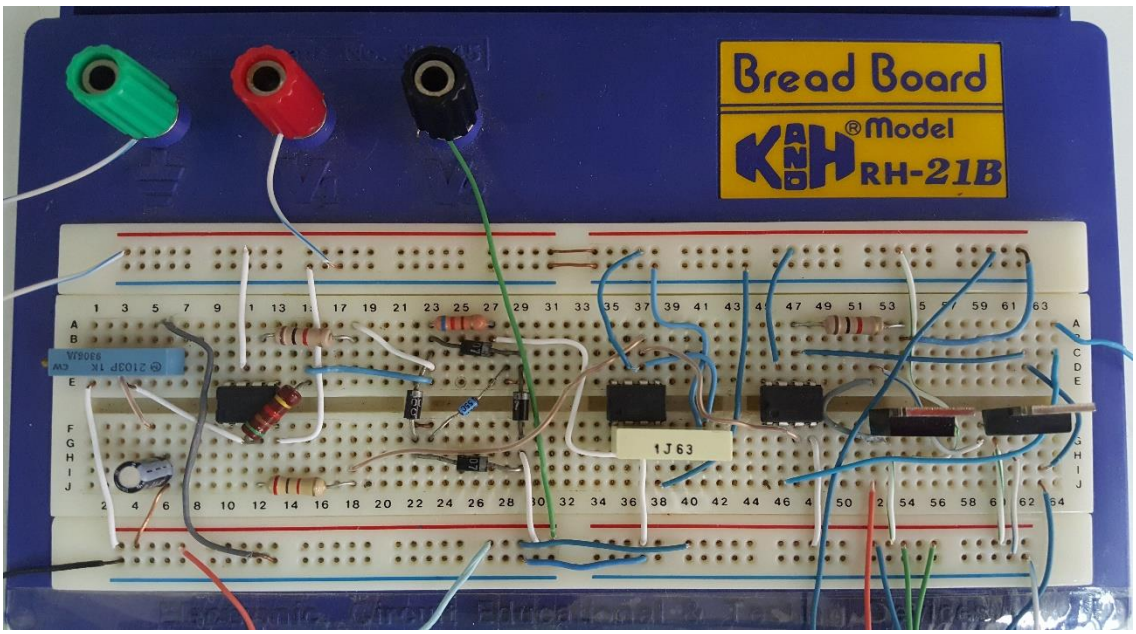

Figure 5. 7: Hardware implementation of the PWM circuit.

Now the design procedure:

The Peak to peak voltage will be seated at 5V ($V_{peak-to-peak} = 5V$) and using eq (5.6) and eq (5.7), we get:

$$\frac{R_2}{R_1} = \frac{V_{peak-to-peak}}{2V_o} = \frac{5V}{2*6.1V} = 0.41 \qquad (5.11)$$

Now by setting $R_1 = 5.1K\Omega \rightarrow R_2 = 2.01K\Omega$.

And by setting $F = 1kHz \rightarrow R = 610\Omega$.

Now V_{ref} will be adjusted for the desired V_a, in this circuit the reference voltage and the frequency can be adjusted independently.

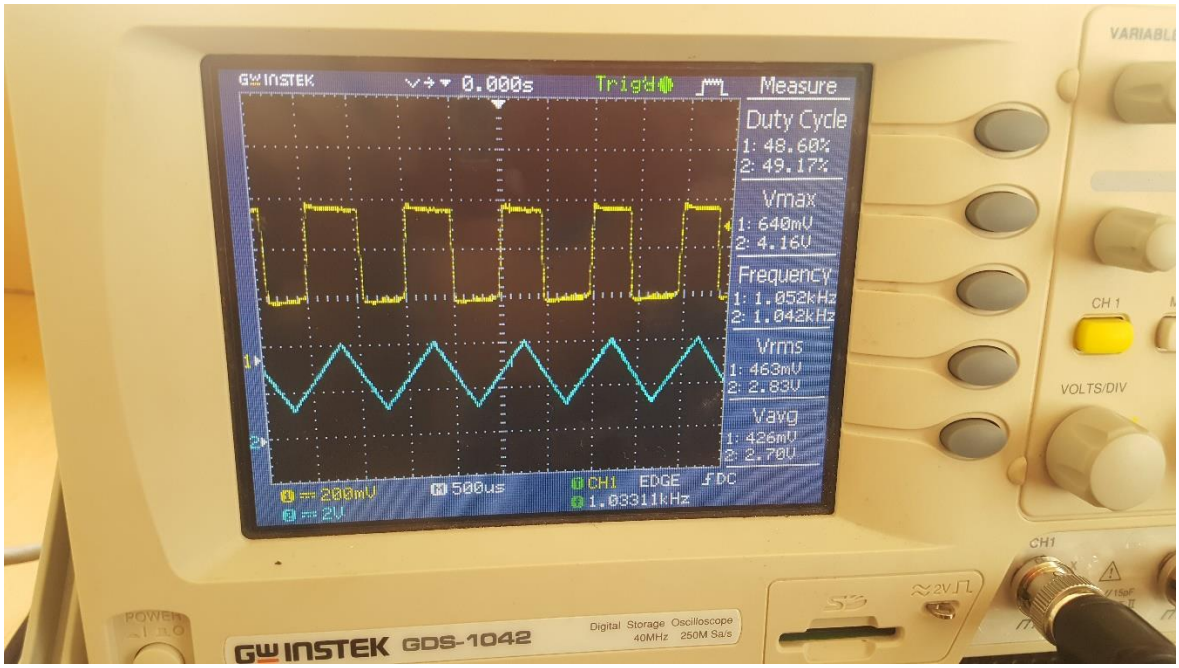

Figure 5. 8: The output graph of the PWM circuit, yellow for output of PWM (square wave) and blue is the triangular wave.

5.3.5 The LABVIEW software

The main part of this project is interfacing of LABVIEW with DAQ NI USB-6009. The designing block diagram and front panel is developed using LABVEIW software. The design is built in order to control the speed of DC motor.

The controller (PID controller) is implemented in LABVIEW with a reference point control as the desired RPM of the motor. The output of the controller which is the voltage of the required PWM is fed to the input of the PWM generator. This PWM signal is then given as the input at the ENABLE pin of IC L293D.

The Block diagram of the virtual instrument for the closed loop PID controller is shown in figure 5.9.

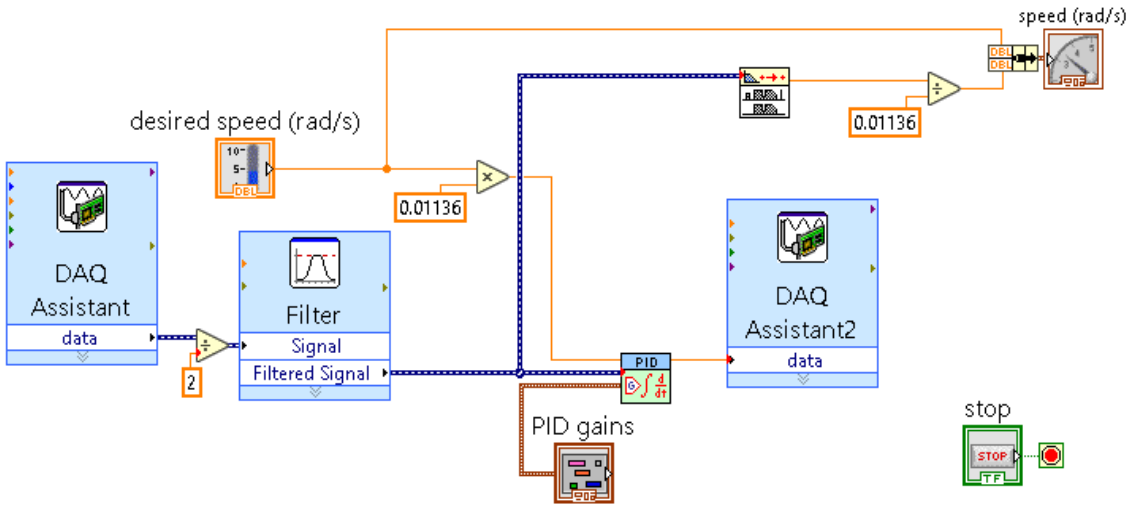

Figure 5. 9: The Block diagram of the VI for the closed loop PID controller.

Figure 5.10 shows the front panel of the virtual instrument for the closed loop PID, This panel will shows the user a gauge that indicates the actual speed and a measuring bar that the user can choose the desired speed. From this, user is able to monitor the environment condition comfortably.

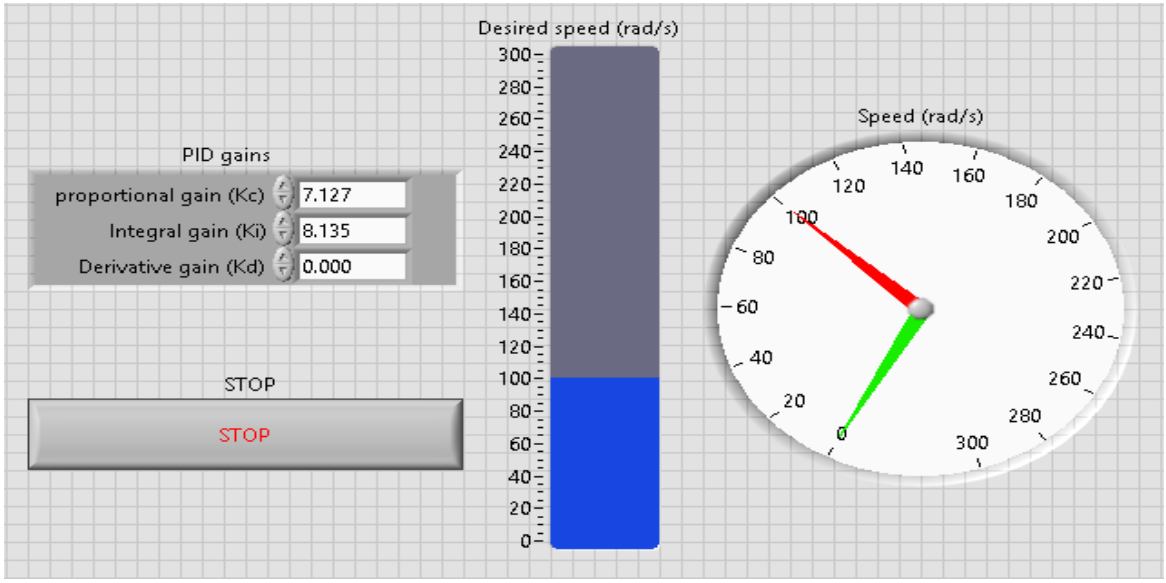

Figure 5.10: The front panel of the VI for the closed loop PID controller.

Duty cycle can be varied from 0-100% by varying the user controlled interactive graphical dial on the front panel. The response of the system can be changed by varying the gains of PID controller. These VI's will be burnt in the DAQ NI USB-6009 and interfaced with the DC motor. Set point, set by the user will be fed into the PID controller and passed on to the DAQ NI USB-6009. PID controller will compare the set point value with the value received from the DAQ. DAQ receives this value from tachometer. Tachometer measures the revolutions of the DC motor. If the two values are not same, PID controller will try to minimize this error and bring the DC Motor to the desired speed.

Figures 5.11 and 5.12 shows the block diagram and the front panel virtual instrument for monitoring the speed, current and torque of the DC motor respectively.

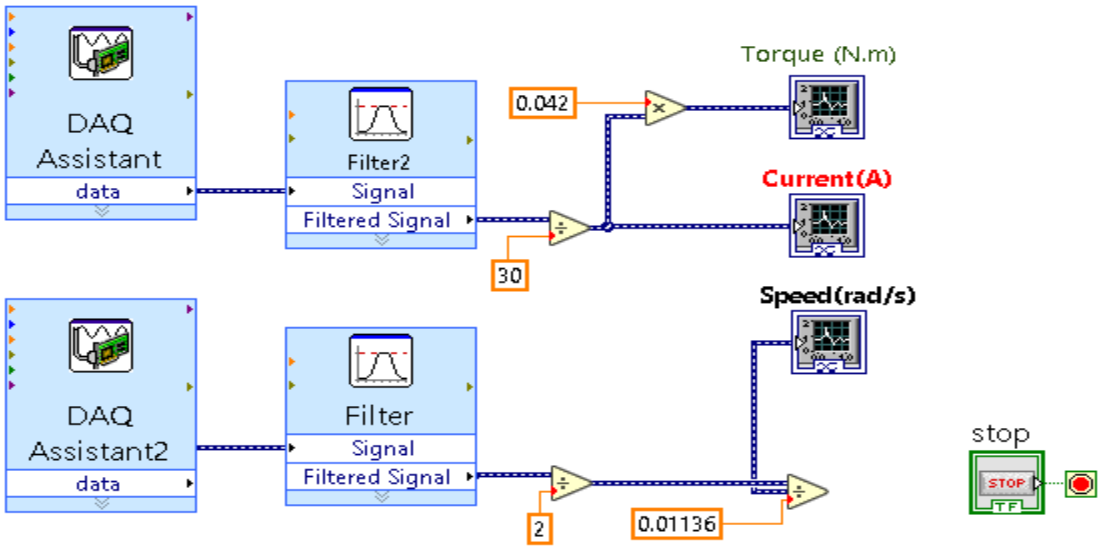

Figure 5.11: VI block diagram for monitoring the speed, current and torque of the DC motor.

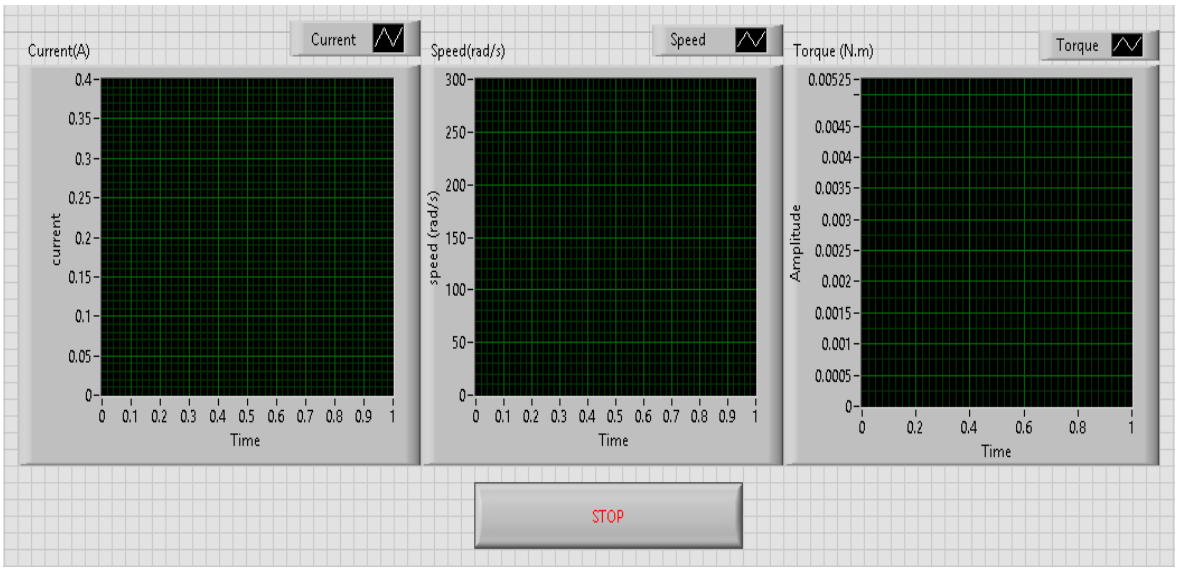

Figure 5.12: VI front panel for monitoring the speed, current and torque of the DC motor.

5.3.6 The over-all setup

Hardware and software required for this project and connections are shown in figures 5.13 and 5.14.

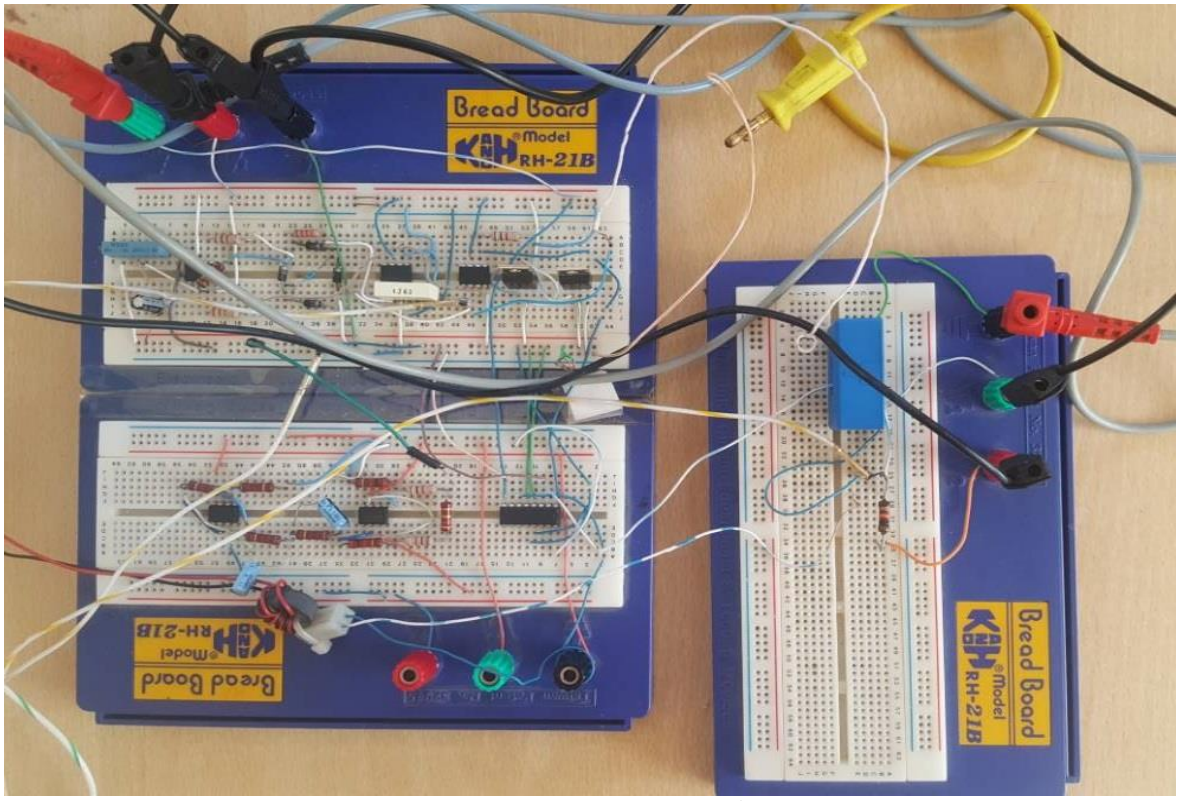

Figure 5.13: The hardware circuit of the system.

The system consists of Hall Effect typed current, torque and speed sensors. Next, all this signals are collected and properly sampled by the heart of the system which is the data acquisition device.

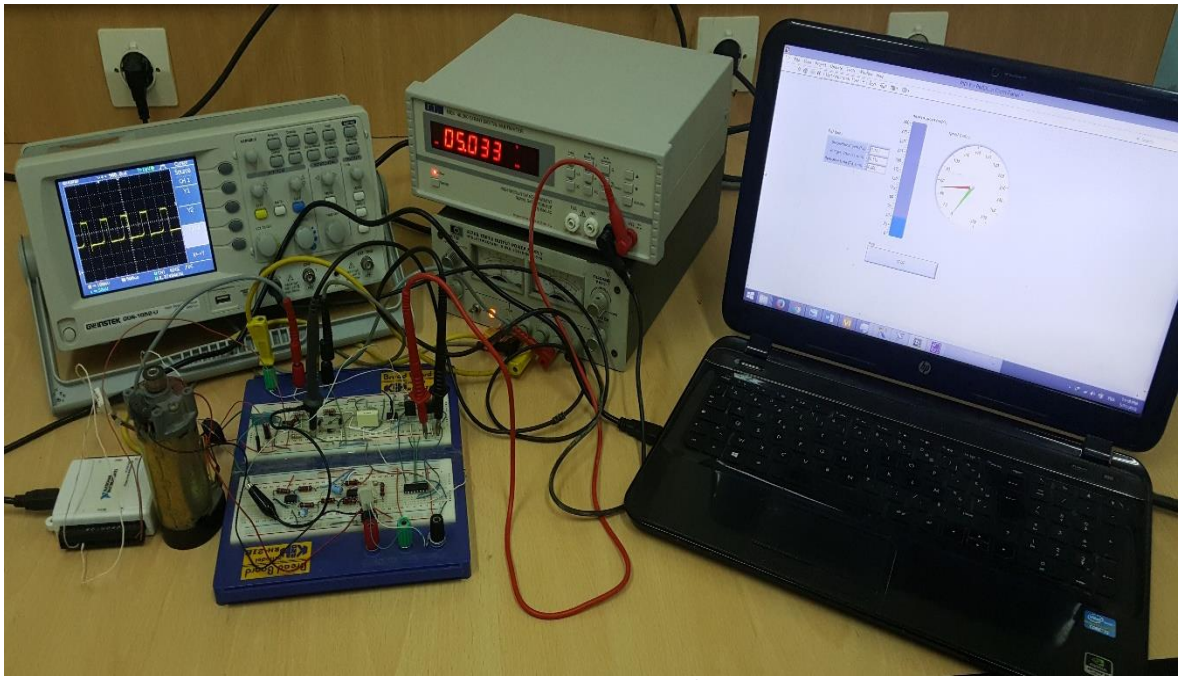

Figure 5.14: The hardware setup of the whole system.

The use of signal conditioning circuit is necessary to be in the operating range of the data acquisition device where the signal is converted into digital form and is acquired by the software (LABVIEW).

5.4 Results and discussion

Various observations were taken for a varied range of inputs (reference rad/s). The following table and graph shows the observations:

Table 5.1: Observation Table for Reference and Observed speed (rad/s).

Reference speed (rad/s)	Output speed (rad/s)
10	23
30	41
50	55
70	74
95	92
100	105
200	192

The results obtained from our current sensing and speed (filter) circuits are shown in the below graphs for a different input voltages.

For an input voltage of 12V:

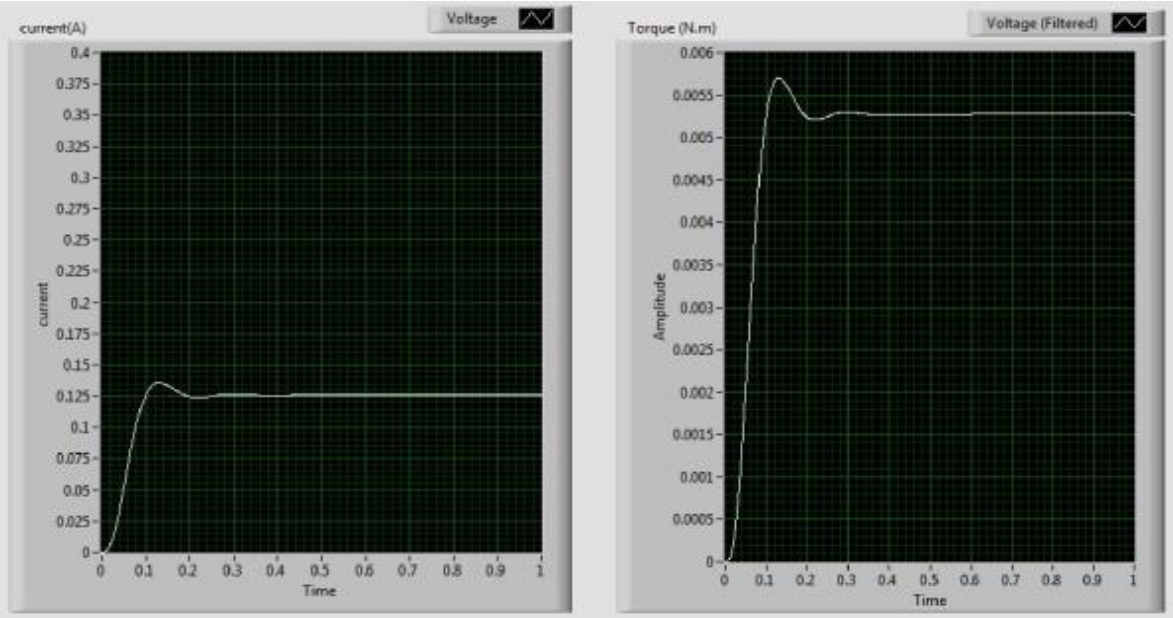

Figure 5.15: The current and torque of the DC motor for an input voltage of 12V.

Figure 5.16: The speed of the DC motor for an input voltage of 12V.

For an input voltage of 3V:

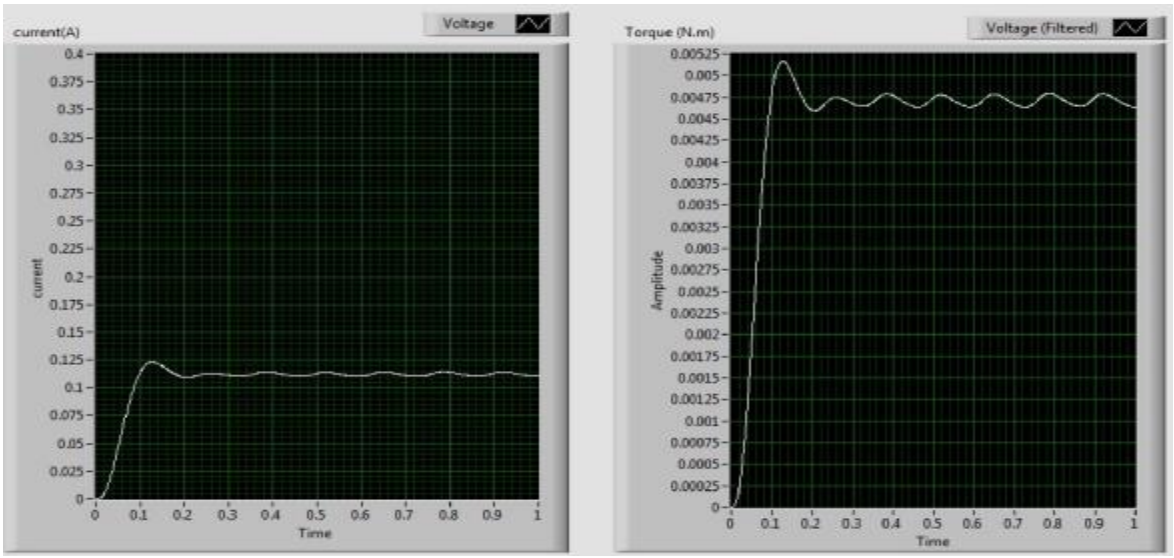

Figure 5.17: The current and torque of the DC motor for an input voltage of 3V.

Figure 5 .18: The speed of the DC motor for an input voltage of 3V.

- The current of the PMDC motor for an input voltage of 12v is 0.125A and the corresponding torque is 0.0053N.m with an overshoot of 4% and the corresponding speed is 260 rad/s.
- The current of the PMDC motor for an input voltage of 3v is approximately 0.125A and the corresponding torque is 0.0046N.m with an overshoot of 7% and the corresponding speed is 45 rad/s.

- The ripple of the torque and speed has been extinguished due the filter action where at high speed the frequency of the ripple is high compared to the cutoff frequency of the filter.
- The ripple of the torque is 0.007 because at low speed the frequency of the current ripple is low compared to that of the high speed and is closer to the cutoff frequency of the filter.
- The duty cycle can be varied from 0-100% by varying the user controlled interactive graphical dial on the front panel. The response of the system can be changed by varying the gains of PID controller.
- The output of the DAQ NI USB-6009 is capable of generating an output voltage 5V so controlling the speed of the PMDC motor at full range will not possible and we are limited at low speeds.
- The experimental results under varying reference speed are shown above. The test shows good results under all conditions employed during simulation.

Conclusion

A brief review of dc drives, choppers, PMDC motors and control theory have been presented in this project report. The speed of a dc motor has been successfully controlled by using chopper as a converter. Proportional-Integral type based Speed and Current controller is used in the closed loop model of DC motor. Initially a simplified closed loop model for speed control of DC motor is considered and requirement of current controller is studied. Then, a generalized modelling of dc motor is done. After that, a complete layout of DC drive system is obtained. Then, design of current and speed controller is done. The simulation is achieved using MATLAB and LABVIEW under different load condition, by varying reference speed condition and varying input voltage. The obtained results are also studied and analyzed under above mentioned conditions. The model shows good results under all conditions employed during simulation such as the proposed PI controller gives better performance and less setting time under the variation of speed and/or load.

After succeeding, in the simulation of speed control of DC motor, it is also implemented in hardware. In this project, the speed control of DC motor is investigated for rated and below rated speed.

REFERENCES

[1] Moleykutty George, "Speed Control of Separately Excited DC Motor". American Journal of Applied Sciences, ISSN 1546-9239, 2008.

[2] Electric Motor Drives, Modeling Analysis and control R.Krishnan.

[3] First_courses_on_power_electronic_and_drives year 2003 edition, Ned Mohan.

[4] Ogata Modern Control Engineering 5th txtbk.

[5] Fitzgerald, Electric Machinery, New York: McGraw-Hill, 2003.

[6] Control Systems Engineering, John Wiley & Sons Inc, 1996.

[7] Control Systems Engineering, Sixth Edition (B.imad).

[8] J. Tang, PID Controller Using the TMS320C31 DSK with on-Line Parameter, 2001.

[9] Sena Temel, "P, PD, PI, PID Controllers".

[10] M. Hadef and R. Mekideche, "Parameter identification of a separately excited DC motor via inverse problem methodology". Turk J Elec Eng and Comp Sci, vol. 17, No.2, 2009.

[11] Adrian V. Bos, Parmaeter Estimation for Scientists and Engineers, First Edition, Wiley, Inc., 2007.

[12] https://en.wikipedia.org/wiki/DC_motor

[13] http://www.profjrwhite.com/system_dynamics/sdyn/s6/s6fintro/s6fintro.html

[14] http://www.profjrwhite.com/system_dynamics/sdyn/s6/s6fmathm/s6fmathm.html

[15] https: // www.researchgate.net/ publication/ 272102820 Parameters Identification of a Permanent Magnet Dc Motor

[16] https://www.electricaleasy.com/2014/12/permanent-magnet-dc-pmdc-motors.html

[17] http://www.completepowerelectronics.com/converters/chopper/

[18] http://www.completepowerelectronics.com/chopper-principle-of-operation/

[19] http://www.completepowerelectronics.com/class-e-chopper-operation/

[20] https://www.slideserve.com/lexi/eeeb443-control-drives

APPENDIX A: Software description

1 NI LABVIEW

NI LABVIEW (Laboratory Virtual Instrumentation Engineering Workbench) is a graphical program (G-programming) development environment from National Instruments (www.ni.com). Programs written in LABVIEW are called VIs (virtual instruments).

One advantage of programming in LABVIEW is that we don't have the overhead to write huge codes. Just the function of the different blocks needs to be known. Also, another advantage is that it works on 'Dataflow Programming' principle, i.e. the output is only obtained when all the inputs get their input data.

LABVIEW consists of two windows called the Front Panel and the Block Diagram.

1.1 LABVIEW front panel:

The LABVIEW front panel is the window where, different controls (such as switch, knobs, numeric inputs, etc.) and indicators (such as LEDs, graphs, numeric outputs, etc.) can be viewed; it can also be called as LABVIEW HMI (Human Machine Interface).

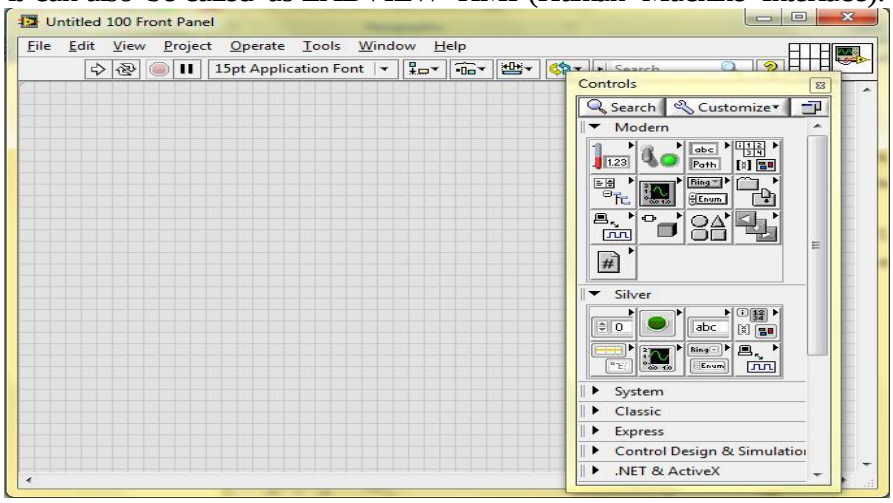

Figure A.1 Front panel window

1.2 LABVIEW block diagram:

LABVIEW block diagram serves as the brain of the program. It contains the graphical source code that defines the functionality of the VI. Front panel objects appear as terminals on the block diagram. The block diagram basically consists of different functions such as mathematical functions, Boolean functions, programming loops, etc.

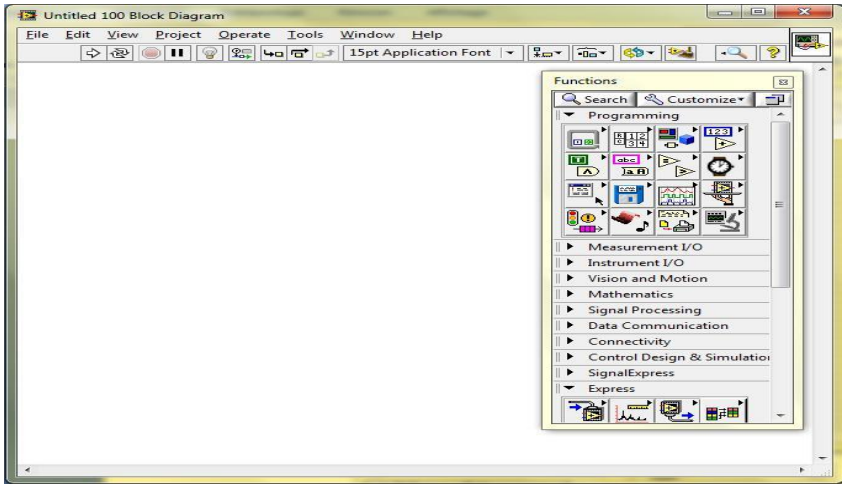

Figure A.2: Block diagram window

LABVIEW program also contains the following three types of pallet which give you the options you need to create and edit the front panel and block diagram:

- **Tools Palette:**

The Tools palette is available on the front panel and the block diagram. A tool is a special operating mode of the mouse cursor. When you select a tool the cursor icon changes to the tool icon. Use the tools to operate and modify front panel and block diagram objects.

- **Controls Palette:**

The Controls palette is available only on the front panel. The Controls palette contains the controls and indicators you use to create the front panel.

- **Functions Palette:**

The Functions palette is available only on the block diagram. The Functions palette contains the VIs and functions you use to build the block diagram. The figure below shows the three types of pallets:

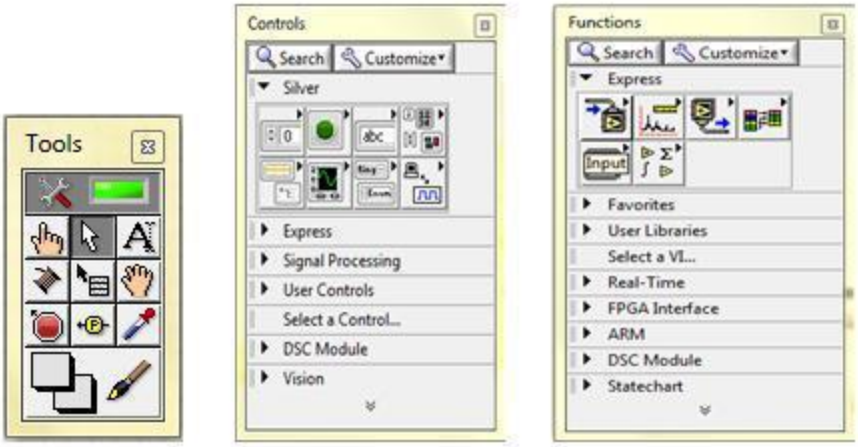

Figure A.3: Tools, Controls and function pallets.

2 Data Acquisition (DAQ)

Data acquisition is the process of measuring an electrical or physical phenomenon such as voltage, current, temperature, pressure, or sound with a computer. The system consists of sensors, DAQ measurement hardware, and a computer with programmable software.

So, Data Acquisition is the process of:

- Acquiring signals from real-world phenomena.
- Digitizing the signals.
- Analyzing, presenting and saving the data.

Lab View software enabled us to acquire data using DAQ board the process block diagram is shown in figure A.4

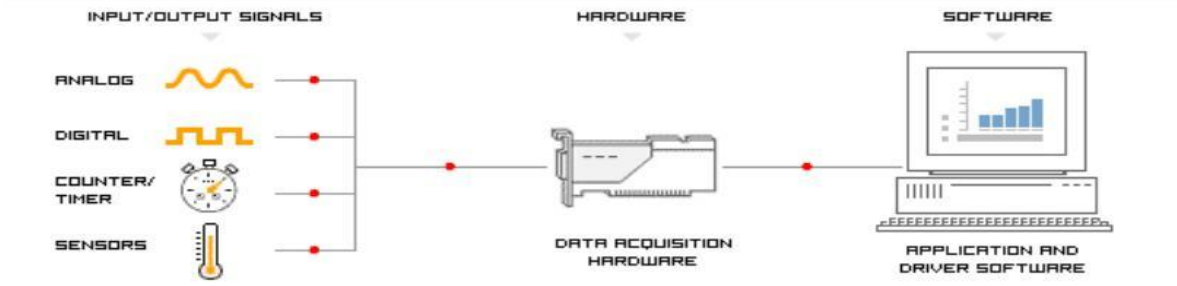

Figure A.4: the process block diagram

The parts are:

1- Physical input/output signals:

A physical input/output signal is typically a voltage or current signal.

2- DAQ device/hardware:

DAQ hardware acts as the interface between the computer and the outside world. It primarily functions as a device that digitizes incoming analog signals so that the computer can interpret them.

3- Driver software and software application:

Driver software is the layer of software for easily communicating with the hardware. It forms the middle layer between the application software and the hardware. Driver software also prevents a programmer from having to do register-level programming or complicated commands in order to access the hardware functions.

Application software adds analysis and presentation capabilities to the driver software. The software application normally does such tasks as: real-time monitoring, data analysis, data logging, control algorithms and human machine interface (HMI).

3 NI-DAQ$_{max}$

Driver software is the layer of software for easily communicating with the hardware. It prevents a programmer from having from having to do register level programming or complicated commands in order to access the hardware functions.

The driver software from national instrument are:

- NI DAQ$_{max}$
- NI DAQ$_{max}$ Base.

The DAQ Assistant, included with NI DAQ$_{max}$, is graphical interactive guide for configuring, testing and acquiring measurement data.

4 DAQ 6009 board

NI USB 6009 is a simple and low cost multifunction I/O device from national instruments.

The device is shown in figure 3.4.1 and has the following specifications:

- 8 analog inputs (14-bit input resolution, 48 ks/s)

- 2 analog outputs (12- bit input resolution, 150 ks/s)
- 12 digital I/O
- USB connection, no extra power, supply needed
- Compatible with labview, labwindows/CVI, and measurement studio for visual studio.NET
- NI_DAQ$_{max}$ driver software.

Figure A.5: NI USB 6009.

4.1 Using NI USB 6009 in LABVIEW

The DAQ$_{max}$ functions, are used in order to use the NI USB6009 in lab view as shown in the figure A.6

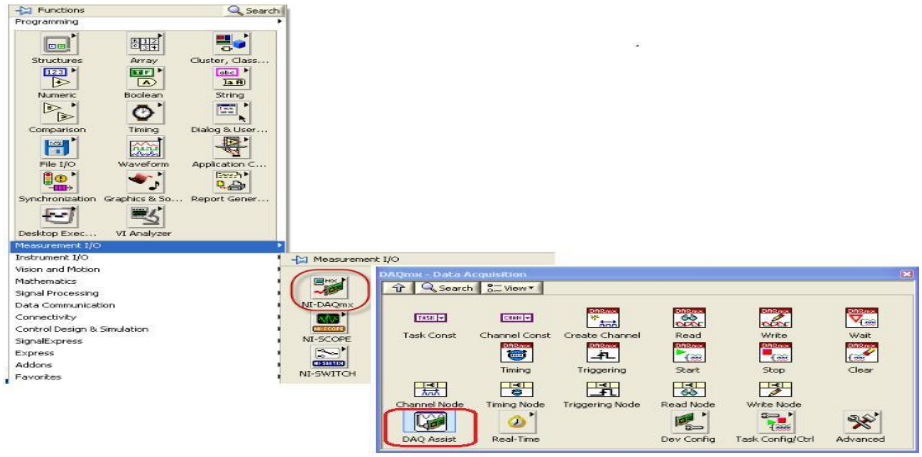

Figure A.6: DAQmax DATA acquisition palette.

By dragging the DAQ assistant icon, a block diagram appears in order to select either « Acquire signals» or « generate signals ». In the next window the type of the input analog

and the appropriate channel from where the data is acquired are selected all these steps are shown in figure A.7

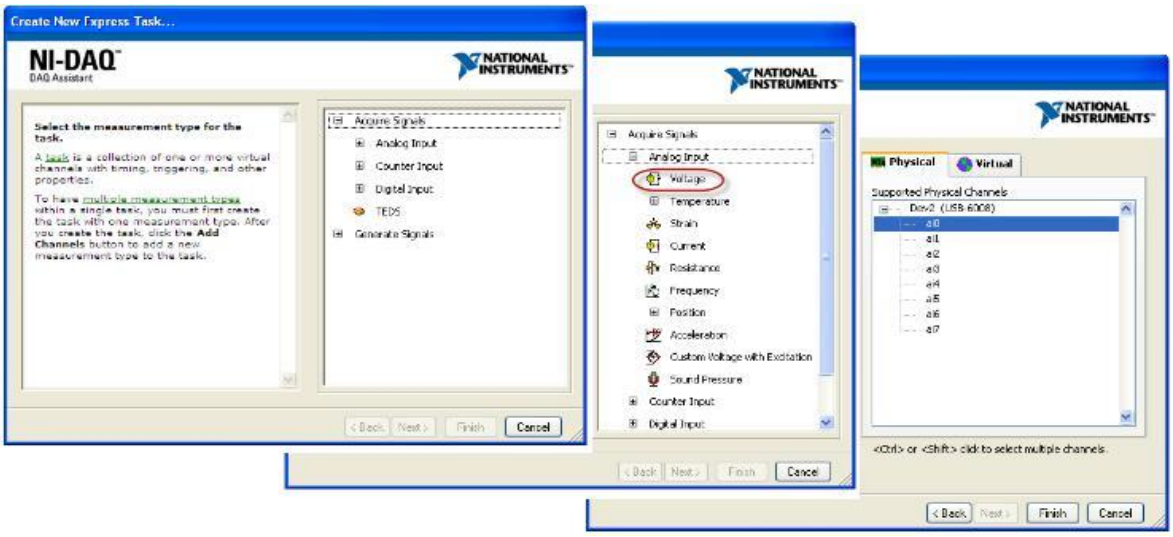

Figure A.7: Setting the DAQ Assistant

In order to acquire the needed data correctly, the DAQ Assistant also allow the user to select the acquisition mode, the signal input range, rating frequency and rename the name of the channels, as in figure A.8

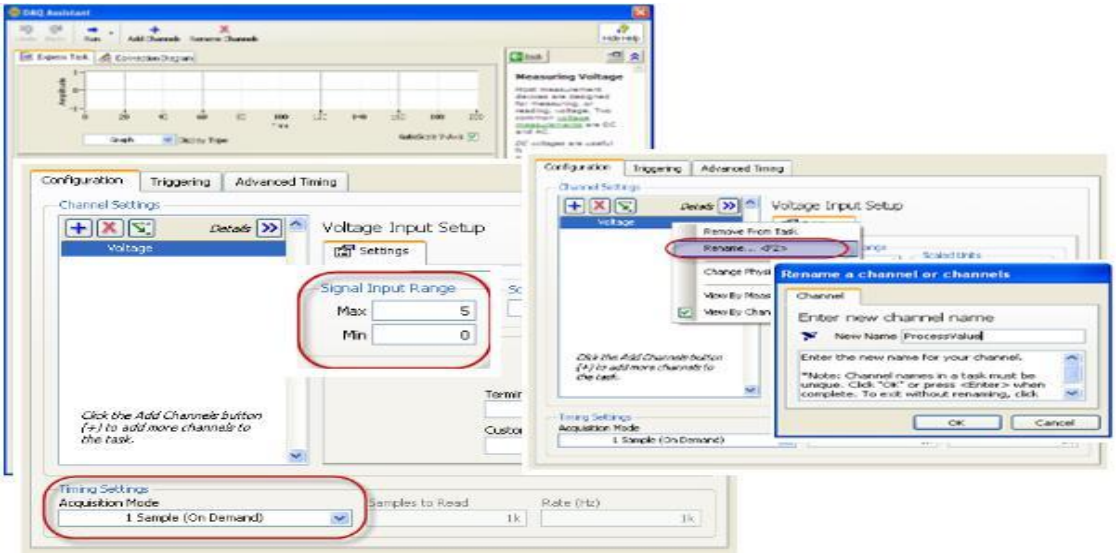

Figure A.8: Different setting to record the data

In this part we are going to record three analog inputs which are voltage, current and speed as explained before, once these parameters are recorded, they will be used to calculate the different output powers of the three phase system.

5 Software implementation

Figure A.9 shows the structure block diagram of the data acquisition system.

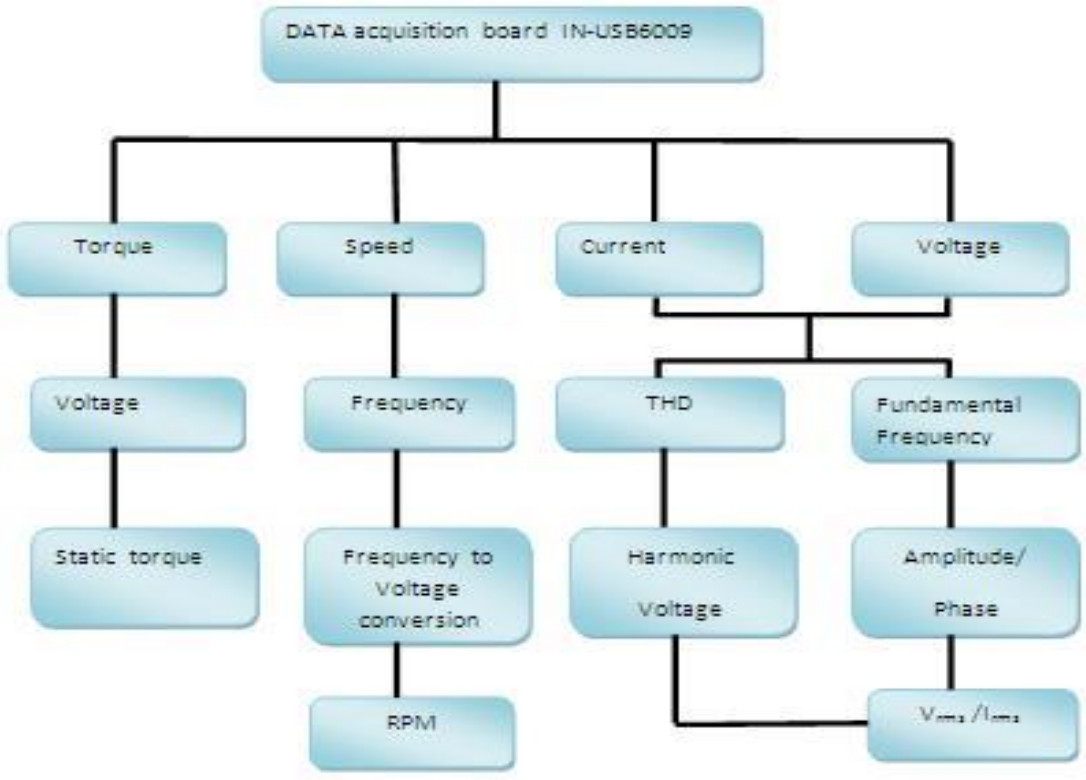

Figure A.9: Data Acquisition block diagram

The DAQ 6009 interface is used to record four different signals namely voltage, current, speed and torque. In order to obtain the rms voltage and current, the Harmonic distortion analyser is used to determine the total harmonic distortion and the fundamental frequency, then from the FFT spectrum (Mag-phase).vi the magnitude and the phase at the fundamental frequency (V_1,I_1) are obtained to find the harmonic voltage and the current.

The revolution per minute (rpm) speed is derived from the conversion of the speed frequency to voltage. In the other hand, the static torque is given by the applied force of the generator.

APPENDIX B: Data sheets

PUSH-PULL FOUR CHANNEL DRIVER WITH DIODES

- 600mA OUTPUT CURRENT CAPABILITY PER CHANNEL
- 1.2A PEAK OUTPUT CURRENT (non repetitive) PER CHANNEL
- ENABLE FACILITY
- OVERTEMPERATURE PROTECTION
- LOGICAL "0" INPUT VOLTAGE UP TO 1.5 V (HIGH NOISE IMMUNITY)
- INTERNAL CLAMP DIODES

SO(12+4+4) **Powerdip (12+2+2)**

ORDERING NUMBERS:

L293DD L293D

DESCRIPTION

The Device is a monolithic integrated high voltage, high current four channel driver designed to accept standard DTL or TTL logic levels and drive inductive loads (such as relays solenoides, DC and stepping motors) and switching power transistors.

To simplify use as two bridges each pair of channels is equipped with an enable input. A separate supply input is provided for the logic, allowing operation at a lower voltage and internal clamp diodes are included.

This device is suitable for use in switching applications at frequencies up to 5 kHz.

The L293D is assembled in a 16 lead plastic packaage which has 4 center pins connected together and used for heatsinking

The L293DD is assembled in a 20 lead surface mount which has 8 center pins connected together and used for heatsinking.

BLOCK DIAGRAM

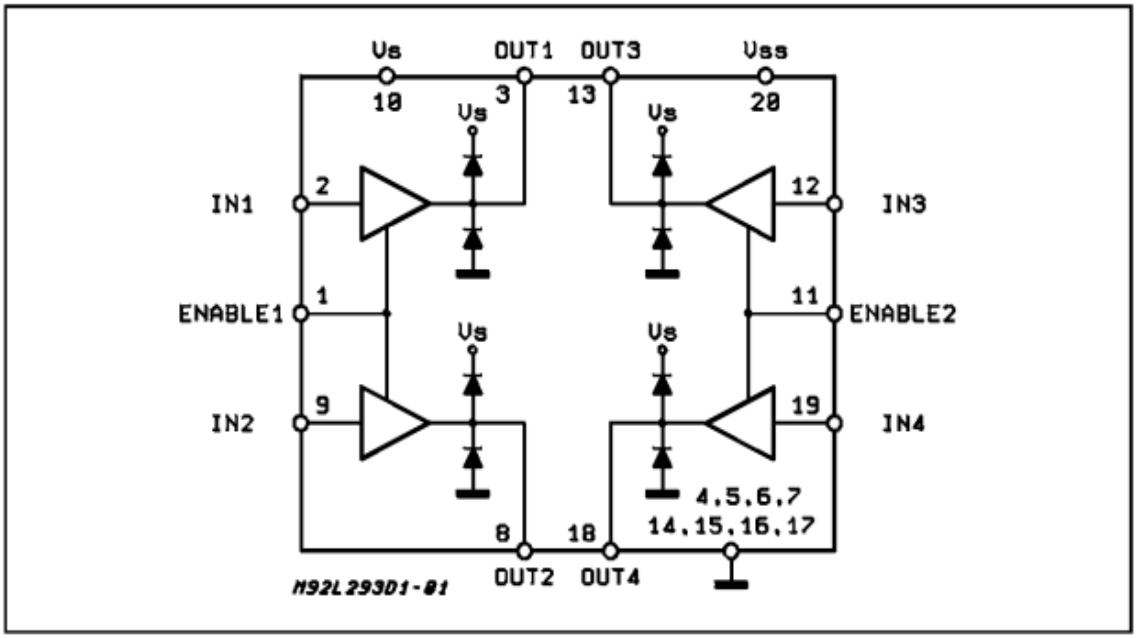

ABSOLUTE MAXIMUM RATINGS

Symbol	Parameter	Value	Unit
V_S	Supply Voltage	36	V
V_{SS}	Logic Supply Voltage	36	V
V_i	Input Voltage	7	V
V_{en}	Enable Voltage	7	V
I_o	Peak Output Current (100 µs non repetitive)	1.2	A
P_{tot}	Total Power Dissipation at T_{pins} = 90 °C	4	W
T_{stg}, T_j	Storage and Junction Temperature	– 40 to 150	°C

PIN CONNECTIONS (Top view)

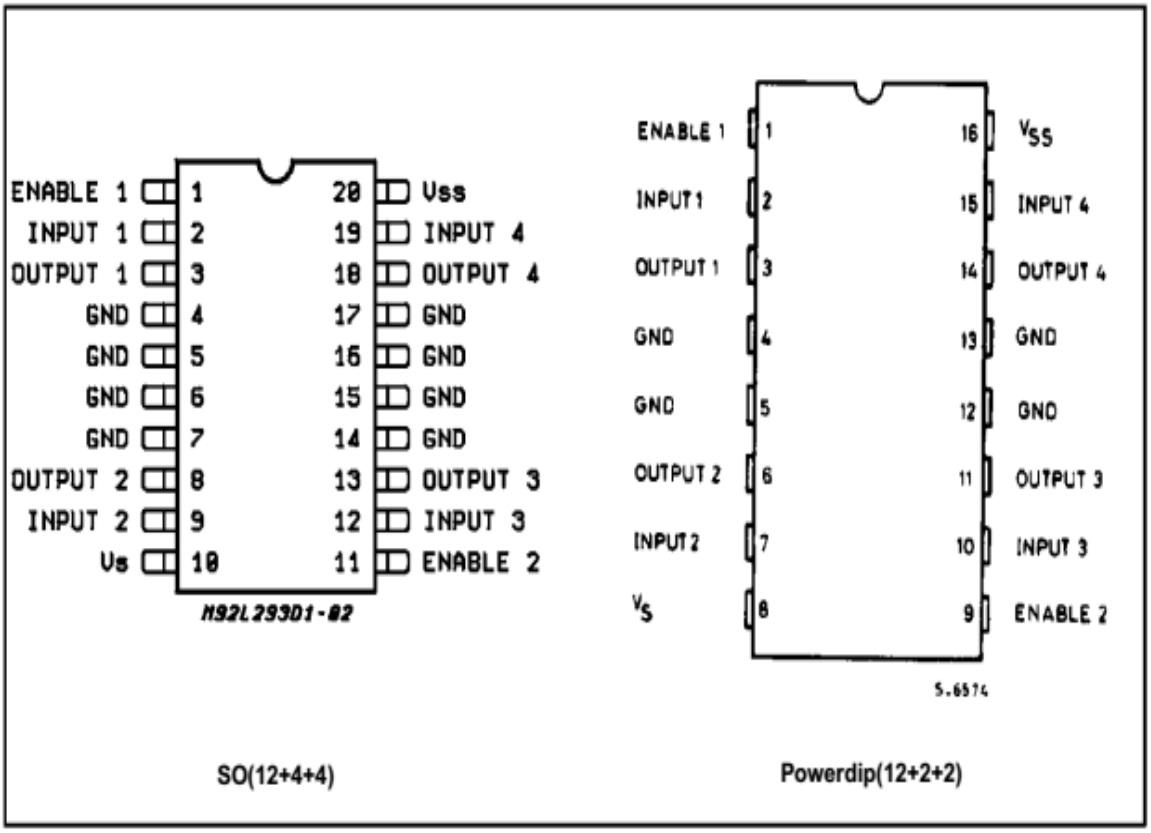

SO(12+4+4) Powerdip(12+2+2)

THERMAL DATA

Symbol	Decription		DIP	SO	Unit
$R_{th\ j\text{-}pins}$	Thermal Resistance Junction-pins	max.	–	14	°C/W
$R_{th\ j\text{-}amb}$	Thermal Resistance junction-ambient	max.	80	50 (*)	°C/W
$R_{th\ j\text{-}case}$	Thermal Resistance Junction-case	max.	14	–	

WIDE BANDWIDTH SINGLE J-FET OPERATIONAL AMPLIFIERS

- HIGH INPUT IMPEDANCE J-FET INPUT STAGE
- HIGH SPEED J-FET OP-AMPs : up to 20MHz, 50V/µs
- OFFSET VOLTAGE ADJUSTMENT DOES NOT DEGRADE DRIFT OR COMMON-MODE REJECTION AS IN MOST OF MONOLITHIC AMPLIFIERS
- INTERNAL COMPENSATION AND LARGE DIFFERENTIAL INPUT VOLTAGE CAPABILITY (UP TO V_{CC}^+)

N
DIP8
(Plastic Package)

D
SO8
(Plastic Micropackage)

TYPICAL APPLICATIONS

- PRECISION HIGH SPEED INTEGRATORS
- FAST D/A AND CONVERTERS
- HIGH IMPEDANCE BUFFERS
- WIDEBAND, LOW NOISE, LOW DRIFT AMPLIFIERS
- LOGARITHIMIC AMPLIFIERS
- PHOTOCELL AMPLIFIERS
- SAMPLE AND HOLD CIRCUITS

ORDER CODES

Part Number	Temperature Range	Package	
		N	D
LF355, LF356, LF357	0°C, +70°C	•	•
LF255, LF256, LF257	–40°C, +105°C	•	•
LF155, LF156, LF157	–55°C, +125°C	•	•
Example : LF355N			

PIN CONNECTIONS (top view)

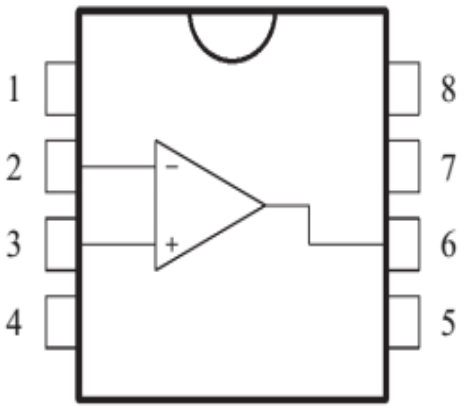

1 - Offset Null 1
2 - Inverting input
3 - Non-inverting input
4 - V_{CC}^-
5 - Offset Null 2
6 - Output
7 - V_{CC}^+
8 - N.C.

DESCRIPTION

These circuits are monolithic J-FET input operational amplifiers incorporating well matched, high voltage J-FET on the same chip with standard bipolar transistors.

This amplifiers feature low input bias and offset currents, low input offset voltage and input offset voltage drift, coupled with offset adjust which does not degrade drift or common-mode rejection.

The devices are also designed for high slew rate, wide bandwidth, extremely fast settling time, low voltage and current noise and a low 1/f noise level.

LM111, LM211, LM311
DIFFERENTIAL COMPARATORS WITH STROBES

SLCS007H – SEPTEMBER 1973 – REVISED AUGUST 2003

- Fast Response Times
- Strobe Capability
- Maximum Input Bias Current . . . 300 nA
- Maximum Input Offset Current . . . 70 nA
- Can Operate From Single 5-V Supply
- Available in Q-Temp Automotive
  - High-Reliability Automotive Applications
  - Configuration Control/Print Support
  - Qualification to Automotive Standards

LM111 . . . JG PACKAGE
LM211 . . . D, P, OR PW PACKAGE
LM311 . . . D, P, PS, OR PW PACKAGE
(TOP VIEW)

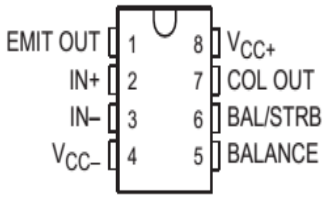

LM111 . . . FK PACKAGE
(TOP VIEW)

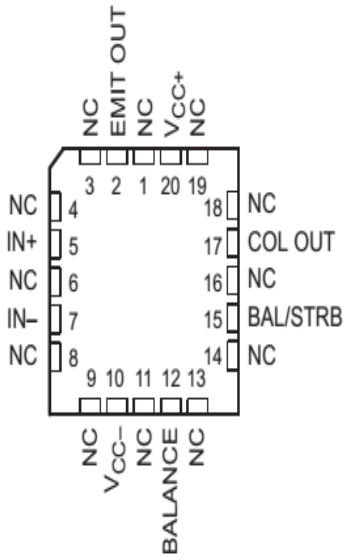

NC – No internal connection

description/ordering information

The LM111, LM211, and LM311 are single high-speed voltage comparators. These devices are designed to operate from a wide range of power-supply voltages, including ±15-V supplies for operational amplifiers and 5-V supplies for logic systems. The output levels are compatible with most TTL and MOS circuits. These comparators are capable of driving lamps or relays and switching voltages up to 50 V at 50 mA. All inputs and outputs can be isolated from system ground. The outputs can drive loads referenced to ground, V_{CC+} or V_{CC-}. Offset balancing and strobe capabilities are available, and the outputs can be wire-OR connected. If the strobe is low, the output is in the off state, regardless of the differential input.

GENERAL-PURPOSE SINGLE OP-AMPs

- LARGE INPUT VOLTAGE RANGE
- NO LATCH-UP
- HIGH GAIN
- SHORT-CIRCUIT PROTECTION
- NO FREQUENCY COMPENSATION REQUIRED
- SAME PIN CONFIGURATION AS THE UA709

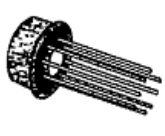

H
TO99
(Metal Can)

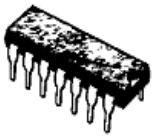

N
DIP14
(Plastic Package)

N
DIP8
(Plastic package)
J
CERDIP8
(Cerdip Package)

D
SO8
(Plastic Micropackage)

GC
LCC20
(Tricecop (LCC))

DESCRIPTION

The UA741 is a high performance monolithic operational constructed on a single silicon chip. It is intended for a wide range of analog applications.

- Summing amplifier
- Voltage follower
- Integrator
- Active filter
- Function generator.

The high gain and wide range of operating voltages provides superior performance integrator, summing amplifier, and general feedback applications. the internal compensation network (6 dB/octave) insures stability in closed loop applications.

ORDER CODES

Part Number	Temperature Range	Package					
		H	J	GC	N	N 14	D
UA741C/E	0 °C to + 70 °C	•	•		•	•	•
UA741I	–40 °C to + 105 °C	•			•	•	
UA741M/A	–55 °C to + 125 °C	•	•	•			

Note : Hi-Rel Versions Available
Examples : UA741CN, UA741IH

PIN CONNECTIONS (top views)

DIP8/CERDIP8
SO8

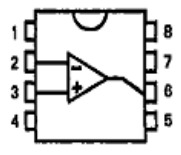

1 - Offset null
2 - Inverting Input
3 - Non-Inverting Input
4 - V_{cc}^-

TO99

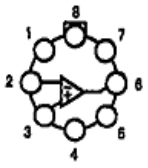

5 - Offset null
6 - Output
7 - V_{cc}^+
8 - NC

LCC20

1 - NC
2 - Offset null
3 - NC
4 - NC
5 - Inverting Input
6 - NC
7 - Non-inverting Input
8 - NC
9 - NC
11 - NC
12 - Offset null
13 - NC
14 - NC
15 - Output
16 - NC
17 - V_{cc}^+
18 - NC
19 - NC
20 - NC

DIP14

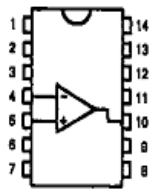

1 - NC
2 - NC
3 - Offset null
4 - Inverting Input
5 - Non-Inverting Input
6 - V_{cc}^-
7 - NC
8 - NC
9 - Offset null
10 - Output
11 - V_{cc}^+
12 - NC
13 - NC
14 - NC

APPENDIX C: The Hall Effect sensor

Current sensor

LEM-25P Hall Effect current sensor is a current transducer, used to measure DC, AC, pulsed …current with galvanic isolation between the primary circuit (high power) and the secondary circuit (electronic circuit). It is also a closed loop sensor.

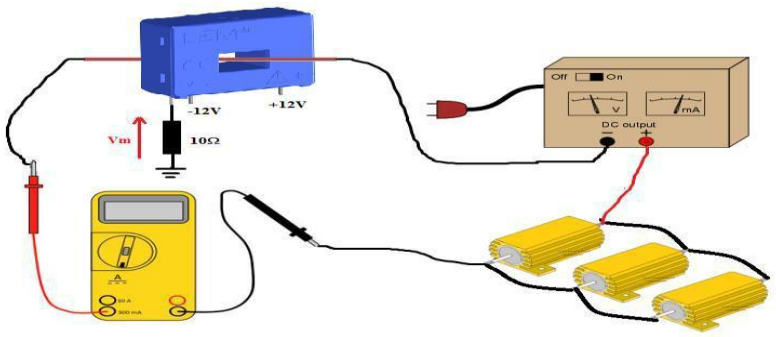

Figure C.1: Supply and testing circuits.

Closed loop sensors amplify the output of the Hall Effect sensor to drive a current through a wire coil wrapped around the core. The magnetic flux created by the coil is exactly opposite of the magnetic field in the core generated by the conductor being measured (primary current). The net effect is that the total magnetic flux in the core is driven to zero, so these types of sensors are also called null balance current sensors. The secondary current in the coil is an exact image of the current being measured reduced by the number of turns in the coil. Passing the secondary current through a load resistor gives a voltage output.

The closed loop sensor has several more components in addition to the core and Hall Effect sensor. The feedback electronics including an operational amplifier and the coil are the significant additions. Figure C.2 shows the construction of a typical closed loop sensor.

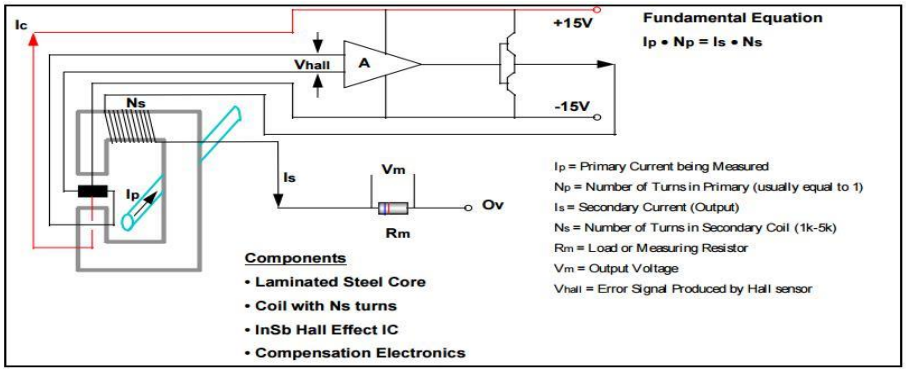

Figure C.2: Construction of a typical closed loop sensor.

The primary current being measured (Ip) creates a magnetic flux in the core. The core is made up of thin pieces of steel stacked together to give high frequency response. The Hall Effect sensor in the core gap measures the amount of flux in the core. The voltage output of the Hall effect sensor is proportional to the current Ip. The output of the Hall sensor is amplified in the compensation electronics. The current output of the compensation electronics (Is) creates a second magnetic field in the coil. The magnitude of this secondary field is the product of current Is times the number of turns in the coil (Ns). The magnetic flux from the secondary coil cancels out the flux from the primary to zero. The system thus operates at zero magnetic flux.

After explaining the principle of the Hall effect current sensor LEM25, we can introduce the design methodology.

Figure C.3: Design methodology for current sensing.